Accepted Manuscript

Miocene to recent extension in NW Sulawesi, Indonesia

Eldert L. Advokaat, Robert Hall, Lloyd T. White, Ian M. Watkinson, Alfend Rudyawan, Marcelle K. BouDagher-Fadel

PII: S1367-9120(17)30367-X
DOI: http://dx.doi.org/10.1016/j.jseaes.2017.07.023
Reference: JAES 3163

To appear in: *Journal of Asian Earth Sciences*

Received Date: 27 February 2017
Revised Date: 3 July 2017
Accepted Date: 14 July 2017

Please cite this article as: Advokaat, E.L., Hall, R., White, L.T., Watkinson, I.M., Rudyawan, A., BouDagher-Fadel, M.K., Miocene to recent extension in NW Sulawesi, Indonesia, *Journal of Asian Earth Sciences* (2017), doi: http://dx.doi.org/10.1016/j.jseaes.2017.07.023

Miocene to recent extension in NW Sulawesi, Indonesia

Eldert L. Advokaat[a, 1]*, Robert Hall[a], Lloyd T. White[a, 2] , Ian M. Watkinson[a] Alfend Rudyawan[a, 3], Marcelle K. BouDagher-Fadel[b]

[a]*SE Asia Research Group, Department of Earth Sciences, Royal Holloway, University of London, Egham, TW20 0EX, United Kingdom*

[b]*Department of Earth Sciences, University College London, Gower Street, London, WC1E 6BT, United Kingdom*

[1]*present address: Department of Earth Sciences, Utrecht University, 3584 CS Utrecht, The Netherlands*

[2]*present address: School of Earth and Environmental Sciences, University of Wollongong, NSW 2522, Australia*

[3]*present address: Geology Study Program, Institut Teknologi Bandung, Bandung, Jawa Barat 40132, Indonesia*

**corresponding author:*

Eldert L. Advokaat

E.L.Advokaat@uu.nl

for: Journal of Asian Earth Sciences

Abstract

The Malino Metamorphic Complex (MMC) in the western part of the North Arm of Sulawesi (Indonesia) has previously been suggested to be a metamorphic complex exhumed in the Early – Middle Miocene. This idea was based on limited K–Ar and $^{40}Ar/^{39}Ar$ age data, but no structural data were presented to provide evidence for the mechanism of exhumation. Here we present new field observations, micro-structural analyses and a revised stratigraphy of NW Sulawesi based on new age data, to provide better constraints on the timing and mechanism of exhumation. The data presented here suggest that the MMC is a metamorphic core complex which underwent lithospheric extension during the Early – Middle Miocene. Although the MMC experienced significant extension, there is no evidence that it was exhumed during this time. There is no contact between the MMC and the Pliocene Ongka Volcanics, contradicting a previously inferred unconformable contact. Pliocene undeformed granitoids intruding the MMC indicate the complex was still at depth during their emplacement. Furthermore, Pliocene and Pleistocene cover sequences do not contain metamorphic detritus. A second phase of extensional uplift was accommodated by brittle faulting from the Late Miocene-Pliocene onwards, during which the MMC was exhumed. This extension is widespread, as indicated by synchronous exhumation of the adjacent Palu Metamorphic Complex in West Sulawesi, and rapid subsidence offshore in Gorontalo Bay. It is linked to northward slab rollback of the southward-subducting Celebes Sea since the Pliocene. GPS data show rapid northward motion of the North Arm of Sulawesi with respect to the Celebes Sea, indicating that this process is ongoing at present day.

1. Introduction

The Indonesian archipelago in the eastern part of the Tethyan region is composed of a complex amalgamation of numerous crustal fragments of various origins. In the west, the Indian Ocean is subducting beneath continental crust of Sundaland. Towards the east, the orogen becomes wider, consists of multiple sutures, and includes more fragments of oceanic and arc origin as well as continental fragments (e.g. Hamilton, 1979; Silver et al., 1983; Hall and Wilson, 2000; Hall, 2009). During the Early Cretaceous, Late Cretaceous and Early Miocene, significant amounts of continental material of predominantly Gondwanan origin were added to the orogen (Hall, 2009; 2011; 2012; Hall and Sevastjanova, 2012) (Fig. 1A), which is one reason why convergence and accretion were long interpreted to be the main mechanisms responsible for its complex geology. However, recent studies in eastern Indonesia have showed that within this convergent zone, there has been widespread Neogene extension (Hall, 2011; Spencer, 2011; Pholbud et al., 2012; Watkinson et al., 2012; Pownall et al., 2013; Pownall et al., 2014; Hennig et al., 2016). Driving mechanisms for this extension include rollback of a slab into the Banda Embayment (Spakman and Hall, 2010).

The K-shaped island of Sulawesi is located in the centre of the eastern Indonesian orogen (Fig. 1B), and comprises four narrow mountainous arms separated by deep bays. Western Sulawesi includes microcontinental fragments of Gondwanan origin, and formed the eastern margin of Sundaland during the Late Cretaceous and Paleogene. The North Arm of Sulawesi is a dominantly Cenozoic intra-oceanic arc built on Eocene oceanic crust (Taylor and van Leeuwen, 1980; Elburg et al., 2003; van Leeuwen and Muhardjo, 2005). Central Sulawesi exposes metamorphic rocks of the former accretionary margin of Sundaland (Parkinson, 1998b), which are overthrusted by a complete, but dismembered, ophiolite exposed in the East Arm (Kündig, 1956; Simandjuntak, 1986; Parkinson, 1998a; Kadarusman et al., 2004). Both Central and SE Sulawesi include blueschists (de Roever, 1950; Helmers et al., 1989), intervening peridotites and other metamorphic rocks (including parts of the Sula Spur microcontinent). This apparently simple configuration of continent, accretionary complex, ophiolite and continent has been interpreted to be mainly the result of convergence and accretion. However, recent studies indicate that extension also played an important role. Exhumed metamorphic core complexes in central Sulawesi were interpreted using SRTM imagery (Spencer, 2010; 2011). Rapid uplift and exhumation of the Palu Metamorphic Complex (PMC) in the Neck of Sulawesi (Hennig et al., 2012; 2014; 2016; van Leeuwen et al., 2016) and synchronous rapid subsidence offshore in Gorontalo Bay (Pholbud et al., 2012; Pezzati et al., 2014a; 2014b; 2015) has been interpreted to be linked to northward rollback of the southward-subducting Celebes Sea under the North Arm during the Pliocene to present-day (Fig. 1B).

The Malino Metamorphic Complex (MMC), in the western part of the North Arm of Sulawesi (Fig. 1B, 2), has been suggested to be a metamorphic core complex exhumed during the Early–Middle Miocene (Kavalieris et al., 1992; van Leeuwen et al., 2007), thus preceding Pliocene extension related to Celebes Sea rollback. However, this interpretation was based on limited field observations, and there are no published microstructural analyses. Only four regional mapping surveys have previously been undertaken, which focussed mainly on the coastal regions and the southern margin of the MMC (Ahlburg, 1913; Koperberg, 1929a; 1929b; Brouwer, 1934; Ratman, 1976), reflecting in part the difficulty of accessing the inland part of NW Sulawesi. Furthermore, the timing of exhumation of the MMC is constrained by only a limited number of widely dispersed K–Ar and $^{40}Ar/^{39}Ar$ ages of 23 – 11 Ma on white mica and hornblende (van Leeuwen et al., 2007), and only a few dates on the volcanic and sedimentary sequences forming the cover of the MMC.

This study presents a stratigraphy of NW Sulawesi, and new age data, field observations and microstructural analyses to constrain the timing and mechanism of exhumation of the MMC in the context of the tectonic evolution of the eastern Indonesian region.

2. Stratigraphy of NW Sulawesi

The following section presents a stratigraphy of NW Sulawesi, which is based on Koperberg (1929a; 1929b), Brouwer (1934), Ratman (1976), Bachri et al. (1994), van Leeuwen and Muhardjo

(2005), in which we incorporate radiometric ages recently published by Advokaat et al. (2014a), Hennig et al. (2016) and Maulana et al. (2016). The reader is referred to the geological map in Fig. 2.

2.1. Malino Metamorphic Complex

Metamorphic rocks which crop out in the Malino Mountains have been assigned to the Malino Metamorphic Complex and comprise Barrovian-type schists and gneisses. Quartzo-feldspathic mica schists to gneisses, locally with feldspar augen, are the dominant lithology, with subordinate garnet schists and amphibolites. Post-metamorphic dykes and stocks intrude the MMC along its western margin (van Leeuwen et al., 2007).

Epidote-chlorite-quartz-bearing greenschists form a discontinuous carapace around the complex. Along the eastern edge, they are derived from basalts of the Papayato Volcanics (Koperberg, 1929b; Kavalieris et al., 1992) and at the western end they are interbedded with marble derived from the Tinombo Formation (Egeler, 1946).

Locally, some additional lithologies have been reported. Andalusite- (and possibly scapolite) bearing quartzo-feldspathic-muscovite gneisses were observed at the confluence of Sungai (river) Molosipat and Sungai Ilotta (Koperberg, 1929b). Quartz veins with tourmaline, and dark graphite bearing garnet-mica schist were found along the Sungai Nasalaa (Ahlburg, 1913; Koperberg, 1929b). Further upstream, Ahlburg (1913) reported the presence of marble lenses enveloped by garnet-mica schists.

Laser ablation inductively coupled plasma mass spectrometry (LA-ICP-MS) U-Pb zircon dating of the schists and gneisses (van Leeuwen et al., 2007) yielded Devonian to Early Carboniferous magmatic ages, and Proterozoic and Archean inherited ages from detrital zircon cores, which were interpreted to indicate an Australian provenance from a location close to the Bird's Head of western Papua New Guinea, based on similarities in age and lithology. Thin metamorphic overgrowths on two grains yielded ages of 19.2 Ma and 17.5 Ma and K-Ar age dating on muscovites from outcrop samples and $^{40}Ar/^{39}Ar$ dating of muscovites and hornblendes from float samples yielded widely dispersed ages between 23–11 Ma (van Leeuwen et al., 2007).

2.2. Paleogene cover formations

The Paleogene formations in the area include the Tinombo Formation (Ahlburg, 1913; Brouwer, 1934) and Papayato Volcanics (Trail et al., 1972). Some authors (Trail et al., 1974; Ratman, 1976; Bachri et al., 1994; Polvé et al., 1997) regarded the Papayato Volcanics as a volcanic member of the Tinombo Formation. van Leeuwen and Muhardjo (2005) showed that the chemical composition of the Papayato Volcanics differs from that of the volcanics in the Tinombo Formation, indicating they were formed in a different tectonic environment, and treated them as separate units. Therefore the nomenclature of van Leeuwen and Muhardjo (2005) is adopted here. The exact relation between these two Paleogene formations is not well-established, but according to Ratman (1976) they might interfinger in the Tolitoli region.

2.2.1 Tinombo Formation

The Tinombo Formation (Ahlburg, 1913; Brouwer, 1934) is a thick, strongly (locally isoclinally) folded sequence of weakly metamorphosed (greenschist grade) sedimentary and subordinate volcanic rocks that is widely exposed in the Donggala Peninsula west of Palu, the northern part of the Neck, and the NW sections of the North Arm. Thickness estimates range between more than 2.5 km along the Tinombo River (GRDC, 1993) and >8 km along the Palassa River (Ratman, 1976). The sedimentary lithologies comprise mainly pelitic rocks (slates to phyllite) with interbedded greywacke, and subordinate radiolarian chert, conglomerate, quartzite, arkosic sandstone, nummulitic limestone, dark dense limestone, and various other calcareous rocks which commonly contain planktonic foraminifera and nannofossils. The volcanic rocks, commonly porphyritic, vary in composition from basalt and andesite, to minor occurrences of dacite and rhyolite (van Leeuwen and Muhardjo, 2005).

The age of the Tinombo Formation is poorly constrained. Based on the presence of nummulitic limestone, Brouwer (1934) demonstrated that the Tinombo Formation is in part of Eocene age. More recent paleontological dating of nummulitic limestone and pelagic carbonates suggests an age range from Middle Eocene to earliest Miocene (Aquitanian)(van Leeuwen and Muhardjo, 2005). Very sparse radiometric dates on volcanic and intrusive members of the Tinombo Formation also indicate an Eocene age (Polvé et al., 1997).

Van Leeuwen and Muhardjo (2005) combined paleontological ages with sedimentary characteristics and suggested that the lower part of the Tinombo Formation, the Middle and Upper Eocene nummulitic limestones, were deposited in a shallow marine environment of lagoons, bars and shoals, whilst the overlying Middle Eocene–lowest Miocene pelitic rocks were deposited in a deeper marine environment affected by turbidity currents.

In the study area, a number of small plutons intrude the Tinombo Formation, which are locally surrounded by contact metamorphic aureoles (Brouwer, 1934; van Leeuwen et al., 1994). The intrusions vary in composition from diorite, quartz diorite, granodiorite and subordinate gabbro and granite (van Leeuwen and Muhardjo, 2005).

2.2.2 Papayato Volcanics

The Papayato Volcanics (Trail et al., 1972) form a 375 km long belt exposed on the North Arm between Ongka in the western part and Kotambagu in the eastern part (Ratman, 1976; Apandi, 1977; Bachri et al., 1994). They comprise a thick series of basaltic pillow lavas and breccias, and less voluminous felsic volcanics which contain rare intercalations of pelagic limestone, radiolarian chert, and greywacke. The association of pillow basalts with interstitial radiolarian chert and pelagic limestone has been interpreted as indicating a deep marine environment with water depths in excess of 500 m (van Leeuwen and Muhardjo, 2005).

The volcanic rocks yielded whole rock K-Ar ages in the range of 50-22 Ma (Polvé et al., 1997). Limited paleontological dating on the sedimentary intercalations indicates an age range between middle Eocene and earliest Miocene (Trail et al., 1974; Rangin et al., 1997; van Leeuwen and Muhardjo, 2005).

The Papayato Volcanics south of the MMC are locally intruded by small orthopyroxene–hornblende andesite stocks, given the name of Bolano Andesite, with a K-Ar whole rock age of 11.6 ± 0.3 Ma (Elburg et al., 2003).

2.2.3 Wobudu Breccia

The Wobudu Breccia (Molengraaff, 1902) crops out along the north coast from the northwestern flank of the Paleleh Mountains to Kuandang Bay in the east. It consists of fragments of andesitic and basaltic agglomerate and conglomerate, tuff ash and lava flows. The agglomerate consists of angular to sub-rounded fragments up to 50 cm across of porphyritic and vesicular basalt and andesite, surrounded by a tuffaceous matrix (Molengraaff, 1902; Trail et al., 1974). South of Kota Paleleh, the Wobudu Breccia consists of massive basic rocks, either basalt flows or minor intrusions. The thickness of the Wobudu Beccia is considered generally only a few hundreds of meters, but near the Bay of Paleleh the estimated thickness is up to 1.5 km (Trail et al., 1974).

The age of the Wobudu Breccia is unknown; the unit lacks fossils and no radiometric ages are available. The assumed age of this unit is inferred from the stratigraphic position above the Dolokapa Formation (Molengraaff, 1902; Trail et al., 1974). The top of the Dolokapa Formation, the Obapi Conglomerate member (Molengraaff, 1902), is dated as Late Miocene to Pliocene, based on an unspecified fossil assemblage (Trail et al., 1974). The Wobudu Breccia should therefore be at least as young as Late Miocene–Pliocene. However, Koperberg (1929a; 1929b) assumed a pre-Burdigalian to Burdigalian age for the Wobudu Breccia based on field relations. Furthermore, a recent study based on extensive fieldwork in the Gorontalo section of the North Arm suggests that the Dolokapa Formation has a smaller extent, and that the formation underlying the Wobudu Breccia might actually be the Papayato Volcanics, which allows a possible older age for the Wobudu Breccia, or even incorporates the Wobudu Breccia into the upper parts of the Papayato Volcanics (Rudyawan, 2016).

2.3. Early Miocene–Pliocene unconformity

An Early Miocene tectonic event was responsible for tilting, folding and thrusting of the Middle Eocene – Lower Miocene volcanic-sedimentary formations. Pliocene–Pleistocene formations rest directly on the Middle Eocene – Lower Miocene volcanic-sedimentary successions (Kavalieris et al., 1992; van Leeuwen and Muhardjo, 2005).

2.4. Pliocene–Pleistocene formations

2.4.1 Coral limestone

Coral limestone occurs on hills with karst topography, up to 500 m high, along the north coast, between Busak, Tanjung (cape) Dako, and the left bank of the downstream part of Sungai Buol (Koperberg, 1929b). Further east along the north coast, isolated outcrops of coral limestone occur between conglomerates of the Lokodidi Formation. The rocks comprise coral limestone, coral breccia with shells of molluscs and marls (Ratman, 1976). Koperberg (1929b) collected samples, which were analysed by Schubert (1913) and yielded a Plio-Pleistocene age.

The presence of coral limestone at elevations of up to 500 m indicates Pliocene–Pleistocene uplift of at least that order (Rutten, 1927).

2.4.2 Lokodidi Formation

Unconformably overlying basement rocks and younger formations are syn- to late orogenic deposits, collectively known as the Celebes Molasse (Sarasin and Sarasin, 1901), which include the Lokididi Beds (Trail et al., 1974; Bachri et al., 1994) on the north flanks of the Paleleh Mountains and the ‘Celebes Molasse of Sarasin and Sarasin’ (Ratman, 1976) in the Buol region. The name Lokodidi Formation is adopted here to include all these units.

The Lokodidi Formation is a sequence of weakly consolidated and poorly sorted conglomerate, quartz sandstone, greywacke, claystone, shale, marl and limestone. The conglomerate consists of components from mainly basaltic and andesitic volcanic and siliceous rocks (Trail et al., 1974; Ratman, 1976; Bachri et al., 1994). Silty claystone and muddy sandstone form beds between 5 cm and 1 m thick in the conglomerate, and contain a few small lenses of limestone with large freshwater (?) gastropod shells. Similar fossils are accompanied by lamellibranch casts in some sandstone beds. Wedge bedding, scour and fill, flow clasts, and intraformational breccia are common in finer sediments near the northern margin of the basin, and indicate deposition from swiftly flowing streams (Trail et al., 1974).

The contact of the Lokodidi Formation with the Wobudu Breccia is difficult to distinguish, and much of the Lokodidi Formation is probably made up by material redistributed from softer upper layers of the Wobudu Breccia (Trail et al., 1974).

The age of the Lokodidi Formation is poorly constrained. The fossil assemblage reported by Bachri et al. (1994) yielded an inconclusive age. The planktonic assemblage reported by Ratman (1976) indicates a Late Miocene to Pliocene age. Limestone and conglomerate layers yielded similar unspecified planktonic assemblages of Pliocene or Pleistocene age (Trail et al., 1974).

2.4.3 Buol Beds

The Buol Beds (van Leeuwen et al., 1994) occur in an area of low elevation southwest of Kota Buol. The base of the Buol Beds consists of massive conglomerates comprised of blocks of rhyolite, tuff, dacite and andesite, interbedded with grits and sandstones (Johnston, 1975). In addition, Koperberg (1929b) reported claystone with some coal seams, marly to calcareous sandstone and conglomerate intercalations, with reworked trachytic and andesitic volcanic material and fragments of foraminifera and *Lithothamnium*. The Buol Beds probably formed during an episode of rapid erosion and deposition (Johnston, 1975) in a small shallow marine basin (Ratman, 1976), which is bordered on the south by faults juxtaposing the Buol Beds and the Papayato Volcanics (Koperberg, 1929b). The Buol Beds are separated by unconformities from the underlying and overlying stratigraphic units (Ratman, 1976).

The age of the Buol Beds is poorly constrained and controversial. Schubert (1913) considered the presence of *Lithothamnium* indicative of an age not older than Miocene, most likely Early Miocene. Ratman (1976) assigned an Early to Middle Miocene age, mainly based on samples with a Burdigalian age described by Schubert (1913) and Koperberg (1929b). These samples are actually located outside the Buol Basin, in the eastern part of the Northern Mountains, an area mapped as equivalent of the Papayato Volcanics by Ratman (1976).

2.5. Neogene igneous rocks

Several plutons and stocks of Neogene age intrude the Malino Metamorphic Complex, Tinombo Formation and Papayato Volcanics.

2.5.1 Late Miocene Series

The Late Miocene Series comprises the Buol Diorite, the Lalos and Bilodondo Plutons and the ‘Younger Series High-K suite’ of Elburg et al. (2003). The Buol Diorite is exposed as hornblende-biotite dacite stocks between Tanjung Lutuno and Busak on the north coast (Koperberg, 1929b). The Lalos Pluton is exposed north of Tolitoli, along the west coast of the Northern Mountains. It comprises coarse grained porphyritic quartz monzonite and coarse grained porphyritic granodiorite, with plagioclase and K-feldspar phenocrysts. $^{40}Ar/^{39}Ar$ dating of hornblendes from the Lalos Pluton yielded a plateau age of 8.2 ± 0.2 Ma (Maulana et al., 2016). The Bilodondo Pluton crops out at several locations along the west coast of the Tolitoli region, as granodioritc pluton intruding the Tinombo Formation. East of Tolitoli, high-K to shoshonitic/ultrapotassic dykes and stocks intruding the Tinombo Formation are reported, which have a K-Ar biotite age of 6.7 ± 0.1 Ma (Elburg et al., 2003).

2.5.2 Pliocene Series

The Pliocene Series comprises the Malino Granitoids and the Ongka Volcanics in the study area, and the Dondo Batholith west of the study area.

The Dondo Batholith comprises biotite granite, quartz monzonite and granodiorite, and is intruded by rhyodacitic dykes and crosscut by several fault sets (van Leeuwen et al., 1994; Maulana et al., 2016). Radiometric dating yielded LA-ICP-MS U-Pb zircon ages of 5.08 ± 0.09 Ma and 5.07 ± 0.10 Ma (Hennig et al., 2016) and K-Ar biotite ages of 4.25 ± 0.10 Ma and 4.12 ± 0.20 Ma (van Leeuwen et al., 1994). Post-metamorphic dykes and stocks belonging to the Dondo Batholith intrude the MMC along its western margin (Ratman, 1976; van Leeuwen et al., 2007), are named here the Malino Granitoids and yielded SHRIMP U-Pb zircon ages of 4.8–3.8 Ma (Advokaat et al., 2014a).

The Ongka Volcanics (van Leeuwen et al., 1994) are exposed in the central parts of the Tobulu mountain range south of the Malino Metamorphic Complex. They comprise poorly consolidated pyroclastics including ignimbrites and subordinate lavas of predominantly rhyodacitic composition, which unconformably overlie the Papayato Volcanics (Elburg et al., 2003). K-Ar whole rock dating yielded ages of 6.23 ± 0.20 Ma (Priadi et al., 1993; Polvé et al., 1997) and 6.7 ± 0.2 Ma (Elburg et al., 2003), but LA-ICP-MS U-Pb zircon ages of 5.0–4.5 Ma (Advokaat et al., 2014a), indicate that the Ongka Volcanics are younger than previously thought.

3. Field observations and microstructures

3.1. Malino Metamorphic Complex

The Malino Metamorphic Complex (MMC) reaches its highest point at Bukit Malino (2448m) (Fig. 2). The complex is bordered on all sides by faults. Only on the western side, a road (Jalan Kotaraya-Tolitoli) crosses the complex. In other parts rivers provide the only access to the complex, typically enabling exploration of only up to 2 km away from the contact zone, except for Sungai Moutong, where a 5 km traverse into the MMC was conducted.

3.1.1 Contact with the Tinombo Formation

The northern contact of the MMC with the Tinombo Formation shows a sinuous curvilinear trend (Fig. 2, 3). Field observations of the northern margin of the MMC were made in the west (along Sungai Silondou and one of its tributaries), and in the central part (along Sungai Ngesgani).

A tributary of Sungai Silondou exposes chlorite schist with a dominant mylonitic foliation oriented between 000/40 and 350/43 (orientation given as dip-direction/dip). Parallel to the foliation, discontinuous boudinaged quartz bands between 0.5-2 cm thick occur within the chlorite schist. At the southern part of the outcrop, the greenschist has a more massive character, with folded quartz bands up to 10 cm thick. Towards the north (in an exposed interval of 20-30 m) the outcrop shows a more planar well-developed foliation increasing in dip to 348/80, with stretching lineations plunging 19/059

ACCEPTED MANUSCRIPT

(lineations given as plunge/azimuth). Several tens of metres to the north a zone of brecciated chlorite schist was observed. North of this outcrop, only intensely deformed rocks belonging to the Tinombo Formation are exposed.

Along the main branch of Sungai Silondou, the first occurrence of massive thin banded greenschist with irregular 5-15 cm thick quartz segregations shows a foliation oriented 014/36. Further upstream, about 500 m to the southeast, abundant quartz segregations marked by stretching lineations plunging 09/028 to 23/008 were observed. Locally, these quartz segregations and stretching lineations are refolded. On the basis of fold vergence and assuming tectonic transport approximately normal to the hinge line, the folds indicate a top-to-the-N sense of shear (Fig. 4A). Pervasive S-C'-fabrics are defined by chlorite mica fish of the S-fabric and oblique, more planar syn-shearing chlorite growth in the C'-fabric. They indicate a top-to-the-north sense of shear (Fig. 4B).

At Sungai Ngesgani, the contact has a more complicated nature (Fig. 5). This river exposes an intensely deformed sequence mainly made up of folded and crenulated muscovite-bearing phyllites belonging to the Tinombo Formation. The crenulation cleavage dips steeply (e.g. 145/72), around a fold axis plunging 16/230. The Tinombo Formation is structurally above greenschists of the MMC. Upstream, towards the MMC, there is a repetition of the sequence of greenschist and overlying muscovite phyllites of the Tinombo Formation. These slices are juxtaposed by brittle normal faults (Fig. 6A-B). The foliation of the greenschist has undulating low angle dips, between 188/16 to 343/30.

South of the inferred major contact zone, mylonitic greenschists are exposed which contain folded and boudinaged quartz bands parallel to the foliation (348/38) (Fig 6C). These quartz bands form strongly lineated and elongated linear sheath folds. Linear elements plunge 39/014 (Fig 6D). South of the greenschists, only coarse grained mylonitic quartzo-feldspathic mica schists were observed at four different outcrops over a distance of 500 m. The outcrops show a similar pattern (Fig. 6E-F): (a) The top of the sequence shows an almost planar foliation dipping ~30° N-NNW. (b) The middle part of the sequence shows tight, localised fold-zones. The vergence of these fold zones indicates a top-to-the-north transport direction. (c) The lower part of the sequence consists of large scale recumbent folds, where the southern limb is steeply (60°-80°) dipping to NNW or SW (d) The southernmost part of the outcrops have similar foliation orientations as those exposed in the uppermost sequence in the outcrop.

Large float in the tributary river consists of the lithologies observed in-situ (quartzo-feldspathic mica schist), as well as garnet-mica schists with garnet porphyroblasts up to 5 cm across. The garnet porphyroblasts are surrounded by a matrix of muscovite, quartz, amphibole, garnet and epidote. In this rock, clusters of garnets also occur. The tributary river extends for about 3 km further into the mountain, therefore these garnet-muscovite schist boulders are assumed to be derived from a proximal source, no further than 3 km upstream from the last outcrop observed.

Float in Sungai Ngesgani also comprises numerous mylonitic quartzo-feldspathic gneiss with large (2–4 cm) K-feldspar porphyroclasts, which indicate a potential plutonic protolith.

3.1.2 Transect around Jalan Kotaraya-Tolitoli

The NW margin of the MMC is exposed in a small stream close to the road from Kotaraya to Tolitoli (Fig. 7). Intensely weathered quartzo-feldspathic mica gneiss with a sub-vertical foliation (123/80) and subhorizontal stretching lineations (05/212) is crosscut by a vertical fault subparallel to the foliation. Slickensides on the fault plane plunge 15/033 and steps on this fault plane indicate a dextral displacement (Fig. 8A-B).

About 150 m to the southeast, mylonitic gneiss is exposed with foliation dipping 325/52 and stretching lineations plunging 45/302. A 1 m wide zone of thin anastomosing shear zones (Fig. 8C-D) with undulating foliations varying in orientation between 330/45 and 330/80 crosscuts the mylonitic gneiss. A steeply NW-dipping brittle fault with slickensides plunging 05/033 juxtaposes the mylonitic gneiss against an undeformed granitoid with large (0.5-3 cm) euhedral K-feldspar crystals, and smaller plagioclase and hornblende crystals, which are surrounded by a fine grained black groundmass. A boulder of float in the river illustrates the intrusive contact relation of the granitoid with the gneisses (Fig. 8E-F).

Along Jalan Kotaraya-Tolitoli, the NW flank of the MMC exposes quartzo-feldspathic mica gneisses with a foliation dipping 120/34. Microstructural analysis reveals S/C’-fabrics which indicate a top-to-the-NE sense of shear. An undeformed granitoid containing 2-4 cm large subhedral to euhedral feldspar crystals is exposed at one outcrop and is assigned to the Malino Granitoids. Quartz-muscovite gneisses and quartzites rest upon the granitoid. Large boulders of hypabyssal intrusive rock were observed about 100 m away from this outcrop, which contain large euhedral crystals of quartz, K-feldspar and plagioclase in a fine grained groundmass.

The crest of the mountains is formed by quartzo-feldspathic mica gneisses with a foliation dipping 229/72. On the southern flank, the foliation undulates, but is dominantly shallow NW dipping. Towards the south the lithologies grade from zoisite-bearing quartzo-feldspathic mica gneiss into epidote-bearing quartzo-feldspathic mica schist with garnet porphyroblasts of ~2 mm across.

3.1.3 Contact with Quaternary alluvium

The SW contact of the MMC consists of an E-W-trending segment which bends around to a SW-NE trend further east. Earlier studies (Ahlburg, 1913; Koperberg, 1929b; Brouwer, 1934) stated that the westernmost occurrence of the metamorphic rocks was along Sungai Molili (Fig. 2, 7), north of Kota Tomini, since west of this river only chlorite schists are exposed.

Sungai Molili exposes a zone of chlorite-epidote schist and boudinaged quartz bands with a gently undulating foliation varying in orientation between horizontal to shallow SE dipping. The chlorite-epidote schist is crosscut by calcite veins (Fig. 9A-B). About 500 m further upstream, chlorite and epidote-bearing garnet-amphibole schists are deformed into a recumbent fold which is crosscut by a fault parallel to the hinge plane. Sigmoidal chlorite tails around garnet porphyroclasts indicate a top-to-the-north sense of shear (Fig. 9C). About 200m upstream, garnet-amphibole schists are juxtaposed against amphibolites and chlorite schists by south-dipping high angle normal faults. Further upstream, the garnet-amphibole schists with foliations undulating between 197/15 to 161/38 are crosscut by a south-dipping (169/16) low angle normal fault associated with a footwall anticline (Fig. 9D).

The SW margin of the MMC comprises a SW-NE-trending segment which exposes a massive ~500 m thick band of greenschist. Along Sungai Mapanga (Fig. 7), the greenschist consists of thin (~1-2 mm) alternating chloritic and quartzitic bands sub-parallel to the foliation dipping 130/58. Quartz bands form discontinuous boudins, truncated by younger shear bands dipping 157/60, with a top-to-the-SW sense of shear (Fig. 9E). Along Sungai Wongiopone dedei (Fig. 7), the foliation is sub-vertical (131/88), with stretching lineations formed by elongated quartz bands plunging 44/221 (Fig. 9F). The outcrop is crosscut by a 1-2 m wide E-W-trending, sub-vertical fault zone. Towards the northeast end of this segment, the foliation of the greenschists has a consistent orientation with the azimuth ranging between 140°-150°, the dip between 25°-40°, and stretching lineations consistently plunge towards 184°-188°. Locally, pods of muscovite phyllite, likely belonging to the Tinombo Formation, occur within the chlorite-epidote greenschists.

The terrain beyond the greenschist was inaccessible, but float samples indicate that the catchment is formed by quartzo-feldspathic gneisses and undeformed granitoids, similar to those observed along Jalan Kotaraya-Tolitoli, suggesting the Malino Granitoids are more voluminous upstream than observed in outcrop.

3.1.4 Contact with the Papayato Volcanics

The southern contact with the Papayato Volcanics is a straight E-W-trending fault zone, which bends towards the south and becomes more irregular towards the east (Fig. 2).

Along the E-W segment, the contact was observed at the Sungai Duyun, a tributary of the Sungai Lambunu (Fig. 10A-B). Basalts of the Papayato Volcanics are exposed south of the contact and are intensely brecciated near the contact. Immediately north of the contact, a ~20-50 m thick band of intensely weathered greenschist with quartz segregations is exposed, foliation dipping 160/54. Slickensides plunge 158/48 on the foliation plane. Coarse grained quartzo-feldspathic mica schist is exposed north of this zone. The foliation is typically 226/40, but does undulate around an axis parallel to the stretching lineation 40/222. Immediately north of this is a zone with alternating amphibolite with thin bands of mica schist and subordinate occurrences of quartzo-feldspathic mica schist with a foliation dipping 177/54, on which mineral lineations plunging 51/200 were observed. Less steep, more SW-ward plunging lineations (36/218) were also observed locally. The northernmost outcrop along Sungai Duyun exposes a K-feldspar augen gneiss with a strongly developed foliation dipping 214/32, and a weakly developed stretching lineation plunging 29/202.

The contact bends more towards the SE at Sungai Sinobulu (Fig. 10C-D). The downstream part of the river exposes massive, dark red to brown basalt, which is brecciated near the contact with the MMC. Immediately north of this brecciated basalt is a ~20-50 m thick unit of epidote-plagioclase-chlorite greenschist with quartz bands with well-developed foliations varying between 188/39 and 223/31 and stretching lineations plunging towards 28/253 (Fig. 11A). Parallel to the stretching lineation, asymmetric isoclinal folds indicate top-to-the-SW sense of shear. Perpendicular to the stretching lineation the foliation undulates in open to close folds without a dominant vergence. Quartz bands in the greenschist show an oblique foliation defined by sub-grain rotation, indicating a top-to-the-SW sense of shear (Fig. 11B). About 100 m north of the greenschist is a zone of amphibole-garnet schist with red weathered quartz bands. These garnet schists have a well-developed foliation dipping 232/25 and a weak stretching lineation plunging 22/213 (Fig. 11C). Round garnet porphyroclasts are commonly 0.5 to 1 cm in diameter and surrounded by a matrix of amphibole, clinozoisite, chlorite and quartz. Chlorite-rich C-fabric shear bands and asymmetric quartz-rich δ-tails of the porphyroclasts indicate a top-to-the-SW sense of shear (Fig. 11D). Another 100 m north is a zone with complex interbanding of amphibolite and quartzo-feldspathic mica schists, characterised by thin banded asymmetric isoclinal folds. The foliation is oriented 233/37, with a stretching lineation of 37/233. North of this zone is a hot spring, where quartzo-feldspathic mica schists to gneisses are exposed. Locally the foliation and a steeply dipping 1-2 m thick quartz vein have been deformed into ~2-5 m open folds, with smaller asymmetric parasitic folds present within (Fig. 11E). The steep limb of this monoclinal fold dips 217/78 and shows a stretching lineation (290/51), while outside the fold the foliation dips 204/37 and the stretching lineation plunges 39/216. Further north the foliation is subhorizontal to shallow north-dipping, with stretching lineations plunging 10/034. S-C' fabrics defined by recrystallized quartz grains and white mica fish indicate a top-to-the-SW sense of shear (Fig. 11F). Vertical E-W-trending, 30-50 cm thick coarse-grained quartz veins crosscut the quartz-mica schists with a regular spacing of about 5 m.

The contact at Sungai Siguru (Fig. 12) is located about 3 km further south relative to the contact at Sungai Sinobulu. The downstream section of the Sungai Siguru exposes predominantly dark red to brown, massive basalt, with minor occurrences of andesite and more felsic lithologies. Towards the contact zone with the MMC, the basalts are crosscut by shallow S-SW dipping joints. North of the basalts is a ~200 m wide zone of fault gouge, first described by Ahlburg (1913), which is weathered to clay masses with varying colours ranging between salmon pink, brown, pale green and red (Fig. 13A-B). Large foliated fragments (Fig 13B) and angular volcanic fragments (Fig 13C) float within this clay mass. At an outcrop immediately north of this zone, the foliation of weathered and brecciated quartzo-feldspathic mica undulates between 183/30 and 199/30 and shows a stretching lineation of 15/240. Greenschist is absent here. Away from this fault zone, quartzo-feldspathic mica schist is the dominant lithology. Locally, the schists contain lenticular quartz veins parallel to the foliation. Stretching lineations on the surface of this quartz vein plunge towards 14/230. The northernmost visited outcrop is approximately 2 km north of the fault zone. Here, the lithology still consists of quartzo-feldspathic mica schists with alternating thin bands of mica-rich layers and quartzo-feldspathic layers (Fig 13D-E). Irregular quartz veins also occur with thicknesses ranging between 1 and 2 cm, and these are oriented parallel to the foliation. The foliation undulates between 188/26, 238/17 and 279/28, around an axis parallel to a strong stretching lineation 13/235 (Fig. 13D). C'-fabric shear bands with a top-to-the-NE transport direction crosscut the schistosity (Fig 13E). Locally, undulating intercalations of lenticular amphibolite bodies occur.

Float in the river comprises lithologies observed in-situ plus garnet schist, with garnet porphyroblasts between 0.5 and 1 cm in diameter, surrounded by a groundmass of amphibole, muscovite and quartz.

At Sungai Moutong and further east, both the basalts of the Papayato Volcanics and the greenschists are absent (Fig. 2). Sungai Moutong exposes quartzites and intensely weathered quartzo-feldspathic mica schists with well-developed S-C' fabrics. Locally, quartzo-feldspathic gneisses with K-feldspar augen are present. In the downstream part of the Sungai Moutong, near the confluence with Sungai Nasalaa, moderately E- to ENE-dipping foliations were observed. Locally, weakly developed stretching lineations plunging 30/017 are present. We did not observe metamorphic rocks further downstream in Sungai Moutong, but Koperberg (1929b) reported foliations dipping moderately to the southeast. At Sungai Olonggala, a river 7 km east of Sungai Moutong, we observed gently east-dipping quartzo-feldspathic gneisses with augen structures.

Between Olonggala and Kota Molosipat, the metamorphic rocks cropping out along the Jalan Trans Sulawesi are intensely weathered thin banded quartzo-feldspathic mica schists, with moderately SE-dipping foliations, and fine grained phyllites comprising thin banded undulating mica-rich layers with discontinuous intercalations of quartzite. The foliation dips steeply towards 136/54, with a weakly developed lineation plunging towards 14/056. On the lower part of the outcrop, lineations were observed both on phyllitic mica schists and on a quartz vein: 17/050.

The most eastern occurrence of metamorphic rock outcrop is along the Sungai Molosipat, north of Kota Molosipat (Fig. 2). Quartzite proto-mylonites with intercalations of epidote-chlorite bands show moderate to steep NE-dipping foliations, with NE plunging stretching lineations.

3.2. Papayato region

Ahlburg (1913) and Koperberg (1929b) reported a deformed (gneissic?) granitoid immediately south of the MMC along the Sungai Molosipat. This granitoid is in fact plagioclase-rich gabbro, which is intruded by dark fine grained andesitic dykes. Both the gabbro and the andesitic dykes show a parallel planar mineral alignment dipping 078/52. The outcrop is crosscut by regularly spaced fractures dipping 195/64.

Along the Sungai Papayato, east of the MMC, an intensely weathered, micro-granitoid is exposed, which has anhedral quartz and anhedral feldspar in fine grained white groundmass. A tributary of the Sungai Papadengo exposes fine grained, vesicular pillow basalt with occurrences of epidote. The float of this river contains mainly mafic igneous rocks (dolerite, andesite and basalt) and some granite, but no metamorphic boulders were observed.

The coastal area between Papayato and Molosipat exposes isolated outcrops of poorly consolidated limestone. The presence of *Migogypsina globulina* in sample STAR12-251 indicates that these fossils originate from Burdigalian reefal sediments (table 1). It is very likely that it is reworked material, since Lower Miocene carbonate deposits are widespread in the central part of the North Arm (Hennig et al., 2014; Rudyawan, 2016).

3.3. Tobulu mountain range

The Tobulu mountain range forms an elevated terrain south of the MMC, and is bounded on the west and SE side by Quaternary alluvial plains (Fig. 2). The northern part of the Tobulu mountain range consists entirely of basalts belonging to the Papayato Volcanics.

At the Sungai Lambunu, fractured, fine grained, dark grey basalt, with small spots of plagioclase and pyrite was observed in-situ. At a small tributary of this river, the float consists exclusively of basalt. Along the road from Moutong via Bolano to Ongka, isolated hills expose pillow basalts, which are crosscut by andesitic dykes about 0.5 m wide, belonging to the Bolano Andesite (Elburg et al., 2003). The southeastern part of the Tobulu mountain range exposes pillow basalts with sediments in the interstitial sites between the pillows. Higher in the sequence, a subhorizontal thin bedded sequence of sandstone and microconglomerate is exposed.

In the central part of the Tobulu mountain range dacitic welded tuffs of the Ongka Volcanics unconformably overlie the basalts of the Papayato Volcanics. Outcrops of the Ongka Volcanics are light grey to white, deeply weathered, poorly cemented and contain white and red weathered lithic fragments of similar composition as the surrounding rock. Outcrops show 1-3 mm large subhedral to euhedral phenocrysts of biotite, feldspar, hornblende, together with angular anhedral fragments of quartz. At the western side of the mountain range, the outcrops are crosscut by E-W-trending subvertical fractures as well as 155°-trending subvertical fractures.

3.4. Tolitoli region

The Tolitoli region is characterised by a ~35 km long, 7 km wide WSW-ENE-trending depression filled by marshes and isolated outcrops of basalts. It is flanked by a 500 m high mountain range to the NW and juxtaposed on the SE by a 060° striking fault to an elevated rugged terrain of similar size. The Tolitoli area is bordered to the south by the MMC and on the north by a linear valley south of Gunung Dako. The area is divided into three geographic units.

3.4.1 South Tolitoli

The rugged elevated terrain immediately north of the MMC exposes mainly intensely deformed sandy shales to slates. In the southwest, the rocks are poorly bedded sandy shales, dipping 162/32. Along Jalan Kotaraya-Tolitoli, a granodiorite intrusion, with large euhedral K-feldspar phenocrysts and smaller biotite and quartz crystals was observed. Adjacent to this granite, the rocks have a more strongly developed slaty to phyllitic appearance, with bedding locally dipping 288/51. The outcrop is crosscut by NNW-trending subvertical quartz-filled fractures.

In the centre of the sub-area, thin bedded slates are more intensely deformed into chevron folds with SSW-NNE-trending, E-dipping axial fold planes and a roughly W-dipping enveloping surface of the bedding (Fig. 14A). The slates are locally intruded by granitoids.

3.4.2 Central Tolitoli

The centre of the Tolitoli region is formed by a marshy depression extending 25 km in WSW-ENE direction and about 5 to 10 km wide. In the centre of this depression, isolated hills expose fine grained vesicular basalts. The outcrop is crosscut by fractures and epidote veins. Towards the eastern end of this valley, pillow lavas (with diameters up to ~1 m) are more dominant. The cores of the pillows are red/brown weathered, the edges and interstices show a green alteration of epidote. At one location, discontinuous intercalations of red mudstone between the pillow lavas were observed (Fig. 14B). Mudstone fills interstices between pillows and overlies pillows. The tops of mudstone intercalations are flat and dip towards 348/85. The mudstone is overlain by laminar auto-brecciated green altered basalt, with calcite veins parallel to the bedding. The top is formed by vesicular basaltic pillow lavas. Foraminifera in sample STAR12-312B yielded a Late Eocene (Bartonian-Priabonian) age range, with an inner neritic depositional environment (table 1).

3.4.3 North Tolitoli

The mountains of northern Tolitoli comprise a core of andesite with adjacent deformed sediments . Along the west coast, granodioritic plutons intrude the sediments.

Near the village of Bilodondo, a granodiorite intruding sediments is exposed, named the Bilodondo Pluton here. The granodiorite is coarse grained, with large (~5 mm) subhedral quartz grains, euhedral feldspar (~2x5 mm) and euhedral amphibole (up to 15 mm). The complex intrusive contact between the granodiorite and the host rocks is sharp and irregular, with a slight decrease in grain size of the intrusion towards the contact. Locally, the host rock rests as a roof-pendant on the pluton (Fig. 14C-E). The pluton is exposed at several locations along the coast over a length of ~15 km. The country rock is black shale to slate with a sub-vertical E-W-trending cleavage. The northern side of the mountains exposes an intensely deformed, thin bedded (2-5 cm), alternating sequence of very fine sandstone and silt. At outcrop scale, deformation increases from north to south.

The core of the mountains is formed by an extensive andesite breccia, with angular fragments ranging in size between 5-20 cm. The matrix consists of large ~5-10 mm subhedral pyroxene and 2-5 mm euhedral/subhedral feldspar in dark grey very fine groundmass.

The SE-side of the mountains exposes a moderately to steeply SE-dipping sequence of alternating sandstone and claystone. The most southern outcrop exposes a steeply SE-dipping sequence of regular alternating thin (~5 cm) light grey indurated claystone beds and darker (volcaniclastic) sandstone. The outcrop is crosscut by a fault 040/74, juxtaposing the sedimentary sequence at the east to basaltic pillow lavas at western part of the outcrop. Further north, a steeply SE-dipping sequence of alternating thin bedded, laminated sandstone and mud/siltstone is exposed. Notable is the presence of a distinctive black, very indurated sandstone layer, which is overlain by a sedimentary breccia composed of angular fragments of the same material in a silt/mudstone matrix. Sample STAR12-302 was collected from this layer, and contained a fossil assemblage with a Burdigalian (N6-N8a) age range.

3.5. Northern Mountains

The Northern Mountains, located on the NW edge of the North Arm, reach the highest point at Gunung Daki (2260 m). To the south WSW-ENE striking linear valleys separate the mountains from the Tolitoli region in the southwest and the Buol region in the southeast. No roads lead into the mountains, so observations were only made along the coastal roads and two river traverses.

3.5.1 West coast

Sungai Lembah Fitra, a northern tributary of Sungai Batu Bota, exposes an indurated black, fine grained rock with a WSW-ENE-trending sub-vertical foliation and discontinuous quartz bands parallel to the foliation. The outcrop is crosscut by closely spaced sub-vertical WSW-ENE-trending fractures. A fault plane is present in the middle of the outcrop. Around this fault plane, the rock is brecciated (Fig. 15A-B). Float in the river consists exclusively of granodiorite, suggesting that the core of the mountains is mostly made of this. Large boulders (metres to tens of metres across) of granodiorite were also observed along the west coast north of Kota Tolitoli.

3.5.2 North coast

Andesite is exposed at the NW corner of the Northern Mountains where it is both massive and auto-brecciated. The western part of the north coast exposes an intensely deformed, alternating sequence of sandstone and mudstone, which shows minor thrusting (Fig. 15C-D) and possible syn-sedimentary slumping. Locally granodioritic stocks intrude this sequence. Between these deformed sequences, isolated occurrences of sub-horizontally bedded limestone crop out. They are packstones containing algae and benthic foraminifera, indicating a reefal environment. The micro-faunal assemblage of sample STAR12-322 yielded a poorly constrained age range between Miocene and Holocene (table 1).

The eastern part of the Northern Mountains exposes a similar intensely deformed sequence of alternating sandstone and siltstone beds, crosscut by SW dipping thrust faults. NW-SE-trending normal faults with small displacements were also observed. The sequence shows a gradual change from sand dominated to silt/mud dominated towards the top. About 3.5 km further to the east similar sequences were observed. Syeno-dioritic stocks intrude the sequence, and are named here the Buol Diorite.

A gently northward-dipping sequence belonging to the Lokodidi Formation was observed, consisting of – from base to top – (a) limestone breccia with mudstone intraclasts and discontinuous recrystallised limestone beds, (c) thin bedded sandy/silty limestone, (d) matrix-supported conglomerate with either a mud/sand matrix or a calcareous matrix and sub-rounded to sub-angular clasts of volcanics, coral fragments and shell fragments. (e) sandy/silty calcareous grainstone with some recrystallised limestone and rock fragments. Forams in coral fragments of unit d yielded a Tortonian (N14-16) age range for sample STAR12-328A and an Early Pliocene age (N19) for sample STAR12-328B (table 1), indicating reworking of material from older formations.

3.5.3 Sungai Buol

Sungai Buol forms the eastern border of the Northern Mountains. The upstream part of Sungai Buol in the south exposes mainly volcanic rocks, including massive andesite and brecciated vesicular basalt. North of these volcanics, fine to medium grained greywacke sandstone is exposed. In some outcrops, this sandstone shows concentric weathering.

In a valley west of Sungai Buol, basalt and microgabbro were observed, crosscut by sets of anastomosing veins and shallow south-dipping faults. Very coarse sandstone with steeply north-dipping bedding is juxtaposed to the basalt. Forams from sandstone sample STAR12-355 indicate a Late Aquitanian-Burdigalian (N5-N6) age (table 1) of deposition in a forereef environment.

The downstream part of Sungai Buol exposes a deformed steeply dipping sequence of alternating thin claystone beds between 5–10 cm thick and sandstone beds between 2–20 cm thick. Several outcrops show evidence of syn-sedimentary slumping, where the lower part of the outcrop is undisturbed, but the upper part is severely disturbed.

In the floodplain of Sungai Buol, an isolated hill exposes a dark grey, fine grained porphyritic igneous rock, which is also interpreted to belong to the Buol Diorite.

3.6. Buol region

3.6.1 Buol Basin

In the southern part of the Buol Province, Koperberg (1929b) observed basalts and radiolarian chert of the Papayato Volcanics, which are juxtaposed against the Buol Beds by faults.

The southernmost outcrop that we visited, exposed a weathered, steeply dipping, alternating sedimentary sequence of (1) matrix supported, fine to medium grained sandy conglomerate with incidental clasts between 5–15 cm and (2) clast supported, very coarse sand to micro-conglomerate with boulders ranging in size from 2–3 cm to 10–15 cm. The clasts contain black mudstone, white mudstone, andesite, basalt and sandstone fragments. In the sandy intervals gastropod fragments were observed.

The central part of the basin exposes a steeply dipping (012/76, overturned), alternating sequence of greywacke sandstone and claystone. Sandstone beds are generally between 5–20 cm thick, claystone beds between 10–70 cm thick. Flame structures at the interface of sandstone and claystone indicate rapid deposition and a younging direction to the south. The sandstone shows wavy lamination of organic-rich layers. In some of the sandstone layers pieces of amber are present. Forams of sample STAR12-349B indicate an inner neritic depositional environment, with a Late Pliocene and Early Pleistocene (N21-N22) age range (table 1).

In the north of the Buol Basin, a gently south-dipping, thin bedded sequence of laminated siltstone with thin intercalations of sandstone beds is exposed. These are unconformably overlain by a moderately NE-ENE dipping sequence of moderately sorted conglomerate belonging to the Lokodidi Formation, with rounded to well-rounded pebbles ranging in size between 1-2 cm up to 20–30 cm. Imbrication of the pebbles indicates a northwards palaeoflow. Some claystone lenses are present, which are overlain by the conglomerate with an erosive base. The clasts include basalt, andesite, mudstone and some dioritic boulders.

3.6.2 Coralline limestones

Coralline limestones are exposed along the north coast up to elevations of about 500 m. They form flat-topped karst topography at Tanjung Dako, the eastern extremity of the Northern Mountains. They fringe the Buol Basin at the north coast and overlie the Wobudu Breccia in the western part of the Paleleh Mountains. Karst topography is recognisable on digital elevation models (DEMs) at Tanjung Dako.

The core of the reef is made up of large (~1 m) radiating corals and locally multiple smaller corals. The rock is very clean limestone, lacking clastic detritus. The reef slope consists of thick bedded, fragmented corals and shells. The forereef is exposed on the SE slope of Tanjung Dako and consists of thin well-bedded limestone with fragments of corals, shells, foraminifera and reworked black volcanics. Sample STAR12-335 was collected here and its micro-faunal assemblage indicates a forereef environment of Early Pliocene age (N19) (Table 1).

Corals of the forereef environment are further exposed in-situ along the north coast between Kota Buol and Lonu at an isolated hill and a more continuous ridge of around 300 m elevation. At Lonu, the limestone contains abundant benthic foraminifera, small broken shell fragments and some larger coral fragments.

3.6.3 Paleleh Mountains

A sequence of siltstone, sandstone and conglomerate belonging to the Lokodidi Formation is exposed between Lonu and Lokodidi. The pebble content is similar to that observed in the northern part of Central Buol, with the addition of sparse quartzite. Locally, this sequence is overlain by recent coralline limestone. East of Lokodidi, thin bedded sequences of alternating sandstone and siltstone are exposed in the vicinity of andesites of the Wobudu Breccia. At one outcrop, they are juxtaposed by normal faults. The andesites occur both as breccia and as massive volcanics. In the latter case, they are exposed as large boulders (core-stones) weathering out of the outcrop. These core-stones are still in-situ, as evidenced by white coarse veins which are continuous both in the weathered part of the outcrop and the boulders. The core-stones contain euhedral, ~0.5 cm pyroxenes and small subhedral feldspar in a grey/greenish groundmass.

Further east the exposed lithologies are mainly andesitic, varying between massive andesite, andesitic breccia, and epiclastic andesitic conglomerates, which are locally intercalated in an sequence of alternating sandstone and mudstone beds.

4. Interpretation of remote sensing data

Van Leeuwen et al. (2007) integrated field observations (Ahlburg, 1913; Koperberg, 1929b; Brouwer, 1934; Ratman, 1976) with high resolution digital elevation models (DEMs) acquired by the Shuttle Radar Topographic Mission (SRTM) (Farr et al., 2007). Here, a new interpretation of 30 m resolution DEMs based on data acquired by the Advanced Spaceborne Thermal Emission and Reflection Radar (ASTER) survey (Yamaguchi et al., 1998) is presented which is integrated with new field observations. The DEM revealed topographic expression of many faults that remained inaccessible during the field mapping campaigns (Fig. 16). The fault systems revealed by the DEM data are described below from north to south.

In the western part of the Northern Mountains, several linear features are recognised which could be interpreted as faults. The first major feature is the Batu Bota Fault Zone (named after Sungai Batu Bota which runs down a significant part of its length), which is recognised as ENE-WSW-trending linear valleys separating the Northern Mountains from terrains of lower elevation in Tolitoli and the southwestern part of the Buol region. In the SW of the Buol region, field observations have confirmed the Batu Bota Fault Zone comprises low angle south-dipping faults, which are locally crosscut by NW-SE-trending strike-slip faults with minor dextral offsets.

In the Tolitoli region a series of ENE-WSW-trending faults of the Talau Fault Zone (named after the river that runs down most of its length) form a marked topographic break between a marsh-filled depression and rugged hills which flank the depression on both sides. Within the graben, several isolated hills demarcated by a 070° trend are present, which are likely to be fault bounded. The Talau Fault Zone runs roughly parallel to the western segment of the northern bounding structure of the MMC.

In the southern part of the Buol region, two sets of faults are recognised: an ENE-WSW-trending set and an E-W-trending set. In the east, the ENE-WSW-trending sets are truncated by the E-W-trending set, while the E-W sets seems to curve around to an ENE-WSW trend towards the west of the area. The fault blocks are characterised by low angle north-dipping facets and steeper south-dipping facets. Based on studies in the Basin and Range province, where the steep side of the fault blocks is the dip slope of the fault, it is suggested here that most of the faults are south-dipping, which is consistent with the south-dipping Batu Bota Fault Zone.

The northern bounding structure of the MMC has a strong topographic expression, juxtaposing the corrugated and incised northern flank of the Malino Mountains against rugged terrain of lower elevation. The bounding structure comprises different segments, which are from west to east respectively a NE-SW-trending steeply dipping segment, curving around into a W-E-trending low angle north-dipping segment, with local outliers (extensional klippen?) consisting of greenschist and cover rocks (phyllites of the Tinombo Formation). In the east the MMC is locally overlain unconformably by elevated areas of low relief, which are interpreted as former intramontane lakes of Quaternary(?) age. The eastern lake is largely intact, whilst the western lake is dissected by faults and incised by river valleys, suggesting it is probably older.

There is some evidence for late stage faulting within the MMC. In the southeastern part, a linear valley in which Sungai Molosipat flows crosscuts the MMC, perpendicular to the foliation and the contact between the MMC and the cover rocks. The valley continues further east into hills where the Papayato Volcanics are exposed, and is therefore interpreted as a late stage (high angle) normal fault, here given the name Molosipat Fault.

The southern boundary of the MMC is formed by several faults. The easternmost segment is the sinuous, SE-NW-trending Siguru Fault. The central segment is an E-W-trending linear high angle normal fault. In this segment there is a curve near the western part of the MMC where the fault becomes a subvertical oblique fault. Here, triangular facets on the lower part of the slopes are recognised. In the western end of the complex, the fault curves back to an E-W-trending south-dipping high angle normal fault and continues further westwards along the coast at least to Palasa. This southern fault zone truncates the northern bounding structure in the west, which indicates that the southern fault was active later than the northern structure.

Roughly parallel to the Siguru Fault, an E-W-trending south-dipping normal fault through the Tobulu mountain range was interpreted by Pholbud et al. (2012), here given the name Tobulu Fault.

5. Discussion

5.1. Revised stratigraphy

Our field observations and new age constraints necessitate minor revision of the stratigraphy of NW Sulawesi (Fig. 3). Lower Miocene clastic sediments are locally preserved in the Northern Mountains. We treat these sediments as a separate unit. The age of the Buol Beds has changed significantly. Previously an Early–Middle Miocene age was assumed (Schubert, 1913; Ratman, 1976) but our new biostratigraphic ages show that the Buol Beds are of Late Pliocene–Early Pleistocene (N21-N22) age.

5.2. Nature of the metamorphic basement exposed in the MMC

Early studies (Koperberg, 1929a; 1929b; Ratman, 1976) suggested that the MMC is an autochthonous antiformal inlier of basement rocks, but van Leeuwen et al. (2007) dismissed this idea based on the tectonic nature of the contact between the MMC and the overlying Tinombo Formation and Papayato Volcanics.

Another hypothesis envisages the MMC as an Australian-derived microcontinental fragment subducted during the Late Oligocene – Early Miocene (van Leeuwen et al., 2007), and exhumed by deep crustal channel flow (Chemenda et al., 1996), similar to a model proposed for the High Himalayan Crystalline Sequence (Searle and Szulc, 2005). In such a scenario, the MMC would have been subducted below the North Arm, and have experienced blueschist or UHP metamorphic conditions. The upper contact between metamorphic rocks and cover sequences would be a normal fault (equivalent to the South Tibetan Detachment), whilst the lower contact between the metamorphic rocks and the subducting slab is a thrust fault (equivalent to the Main Central Thrust) with an inverted Barrovian metamorphic field gradient. There is little field evidence to support this scenario; although the lower contact was not observed in the field, (a) kinematic indicators on the contact with the cover formations show both top-to-the-north and top-to-the-south shearing, whereas uni-directional shearing would be expected in the case of channel flow, and (b) the dominant amphibolite facies mineral assemblage and the presence of granites is similar to Barrovian metamorphism (van Leeuwen et al., 2007) with a normal metamorphic field gradient on both sides of the complex, contrary to the inverted field gradient expected near the southern contact.

Previous authors have suggested that the MMC is an extensional metamorphic core complex (Kavalieris et al., 1992; van Leeuwen et al., 2007). Our field observations support this concept: (a) the MMC has an elongated dome shape with metamorphic grade increasing towards the core of the complex (Figs. 2, 17), (b) mylonitic shear zones with kinematic indicators displaying normal sense extensional shearing form a distinct contact between high grade metamorphic rocks and low grade and unmetamorphosed cover sequences, equivalent to the detachment surface of a metamorphic core complex, (c) late stage granite magmatism is indicative of LP-HT conditions, (d) there is late stage high angle normal faulting, commonly observed in core complexes in the eastern Mediterranean (e.g. Hinsbergen and Meulenkamp, 2006; Cavazza et al., 2009; Advokaat et al., 2014b), and (e) the cover sequences are attenuated by normal faults.

5.3. Neogene tectonic scenario for NW Sulawesi

Based on our new field observations, structural data and age constraints, combined with previous observations, age constraints and models, we present a scenario for the Neogene tectonic evolution of NW Sulawesi.

5.3.1 Late Oligocene–Early Miocene collision of the North Arm and the Sula Spur

The stratigraphy of NW Sulawesi is characterised by an Aquitanian unconformity and a Pliocene unconformity, where the latter erodes down to the Burdigalian. An Aquitanian deformation event was responsible for tilting, folding and thrusting of the Middle Eocene–earliest Miocene volcanic-sedimentary formations. $^{40}Ar/^{39}Ar$ hornblende plateau ages of ~23 Ma, and metamorphic zircon overgrowths of 19.2 Ma and 17.5 Ma also hint at a metamorphic event, during which the MMC experienced greenschist facies to epidote-amphibolite facies and upper-amphibolite facies Barrovian-style regional metamorphism, with peak metamorphic conditions of 7.5 – 9.6 kbar at 646 – 671 °C (van Leeuwen et al., 2007). Following this event, shallow marine sedimentation in NW Sulawesi resumed in the Burdigalian.

Contemporaneous Late Oligocene–Early Miocene deformation and metamorphic events are recognised throughout Sulawesi, which are linked to a collision of a microcontinental fragment, now identified as the Sula Spur, with the eastern margin of Sundaland (Silver et al., 1983; Hall, 2002; 2012; Spakman and Hall, 2010).

In west Central Sulawesi, along the Palu-Koro Fault (Fig. 2), garnet peridotite and associated high grade metamorphic rocks crop out. Helmers et al. (1990) provided estimates of peak metamorphic conditions of 11.5–13 kbar and 750–800 °C for felsic granulites, and 15–20 kbar and 1050–1100°C for garnet peridotite. Sopaheluwan et al. (1995), Kadarusman and Parkinson (2000), Kadarusman et al. (2002; 2005; 2011) and van Leeuwen et al. (2016) reported additional lithologies including mafic granulite, eclogite and garnet lherzolite. Mafic granulite recorded PT conditions of 10–16 kbar and 700–850 °C. Eclogite recorded peak metamorphic conditions of 20 kbar and 1060 °C, and decompressional cooling to 10–12 kbar and 750–870 °C. The garnet lherzolite recorded peak metamorphic conditions of 26–38 kbar and 1025–1210°C, and near-isothermal decompression to 4–12 kbar at temperatures 50–240°C below peak metamorphic temperatures (Kadarusman and Parkinson, 2000; Kadarusman et al., 2002; 2011). Kadarusman et al. (2001; 2011) reported Sm-Nd garnet ages from garnet peridotites, in which the core of the garnet records peak metamorphism at 27.6 ± 1.13 Ma, whilst the rim of the garnet records a cooling age of 20.0 ± 0.26 Ma. The Palu-Koro peridotites were interpreted to represent a mantle wedge fragment of Sundaland sub-continental lithosphere (Kadarusman and Parkinson, 2000), which is linked to the collision of the Sulu Spur microcontinent with the eastern margin of Sundaland during the Late Oligocene–Early Miocene (Kadarusman et al., 2001, 2002, 2011; van Leeuwen et al., 2016).

There are no metamorphic rocks in the South Arm of Sulawesi which record a Late Oligocene–Early Miocene event, possibly because the boundary between West Sulawesi and the Sula Spur was a transform margin at this time (Spakman and Hall, 2010; Hall, 2012) (Fig. 2). Volcanic-sedimentary successions in the South Arm are characterised by apparent gaps in the Late Oligocene–Early Miocene, which may be an artefact of sampling, or may represent an erosional event (van Leeuwen et al., 2010). In the Latimojong Mountains, a rhyolite dyke with a SHRIMP U–Pb zircon age of 25.0 ± 0.7 Ma crosscuts Eocene basalts of the Lamasi Complex, indicating there was some latest Oligocene–earliest Miocene arc volcanism (White et al., 2017).

5.3.2 Early – Middle Miocene lower crustal extension in NW Sulawesi

Top-to-the-north extensional shear zones are observed throughout the MMC. We interpret them as supra-core complex extensional detachments related to lithospheric thinning. It is possible these detachments were localised along pre-existing deep thrust systems related to the Sula Spur collision. Reactivation of former thrust faults is commonly observed in metamorphic core complexes (Platt and Vissers, 1989; Forster and Lister, 2009; Lister and Forster, 2009). Top-to-the-south extensional shearing is restricted to the southern margin of the MMC. Although there is evidence for lithospheric extension during the Early – Middle Miocene, as suggested by K-Ar and $^{40}Ar/^{39}Ar$ ages of 23 – 11 Ma on white mica and hornblende (van Leeuwen et al., 2007), there is no evidence that the MMC was also exhumed at this time, since our field observations show that (a) the MMC is not in contact with the Ongka Volcanics, contradicting the inferred unconformable contact as mapped by Ratman (1976) and van Leeuwen et al. (2007), (b) undeformed Pliocene granitic stocks of the Malino Granitoids which intrude the MMC postdate ductile shearing and indicate that the MMC was still at depth during their time of emplacement, and (c) Pliocene–Pleistocene sediments (Coral Limestone, Buol Beds, Lokodidi Formation) lack metamorphic detritus, which suggests either that eroded material was transported elsewhere, or – more likely – the metamorphic rocks were not yet at the surface and thus not available for erosion during deposition of these sediments.

5.3.3 Late Miocene to present day uplift and extension in NW Sulawesi

Rutten (1927) proposed that Lower Pliocene coral limestone found at modern elevations of up to 500 m recorded Pliocene-Pleistocene uplift of at least that order. This uplift was at least in part accommodated by brittle normal faulting. Cross-cutting relations provide some first order constraints on the timing of these faults.

The main part of the Batu Bota Fault Zone (Fig. 16) juxtaposes sediments of the Tinombo Formation to granodiorite of the Lalos Pluton. Maulana et al. (2016) reported an $^{40}Ar/^{39}Ar$ hornblende plateau age of 8.2 ± 0.2 Ma for the Lalos Pluton, and the emplacement depth was estimated at 11.6 km based on Al-in hornblende geobarometry (Maulana, 2013). The Lalos Pluton shows no evidence of significant deformation, and therefore it is assumed that the Batu Bota Fault Zone was active only after emplacement and cooling of this pluton. There are no age constraints for movement on the Talau Fault Zone and the faults in the southern part of the Buol region, but given the similar orientation to the Batu Bota Fault Zone, it is likely that they were contemporaneously active.

The faults in the central Buol Basin are even younger. Sub-vertical Upper Pliocene-Lower Pleistocene (N21-N22) sediments indicate that significant tectonic activity must have occurred after deposition.

There two possible ages for the activity of the Lambunu Fault (Fig. 16). It was active shortly before or during emplacement of the Ongka Volcanics (5.1–4.5 Ma; Advokaat et al., 2014a), and the extent of the ignimbrites was constrained to a (half-)graben by the antecedent topography. More likely the fault was active after emplacement of the Ongka Volcanics. When restoring the fault displacement, the Ongka Volcanics are located roughly above the MMC and the Malino Granitoids (Fig. 17). Their limited spatial extent is explained by subsequent erosion from the uplifted block north of the Tobulu Fault.

The high angle normal faults that mark the southern boundary of the MMC have a similar orientation to the Tobulu Fault and were likely synchronously active. On the western margin of the MMC, they truncate the fault on the NW side of the MMC, indicating that the southern fault was active later.

In stark contrast to the Pliocene-Pleistocene sediments in Buol, Holocene alluvial deposits and present-day rivers carry abundant metamorphic float, suggesting exhumation of the MMC is very recent.

5.3.4 Regional Pliocene to present day uplift onshore and subsidence offshore

Extension and uplift observed in NW Sulawesi occurred in a regional extensional tectonic regime. In the Neck of Sulawesi, high mountains exposes high-grade metamorphic rocks of the Palu Metamorphic Complex (PMC), which are intruded by Late Miocene–Late Pliocene granitoid batholith and are flanked by syn-orogenic sedimentary sequences of Pliocene–Pleistocene age suggesting rapid uplift and exhumation (van Leeuwen and Muhardjo, 2005; Hennig et al., 2016; van Leeuwen et al., 2016). Metamorphic rocks from the Palu Metamorphic Complex (PMC) yielded SHRIMP U-Pb zircon ages on metamorphic rims of 3.67 – 3.12 Ma (Hennig et al., 2016) and $^{40}Ar/^{39}Ar$ plateau ages of 3.8 – 2.0 Ma (van Leeuwen et al., 2016). (U-Th-Sm)/He apatite dating from granitoids in the PMC yielded ages of 2.9 ± 0.4 Ma and 2.4 ± 0.4 Ma. Based on those ages, exhumation rates were estimated at 1-4 mm/yr (Hennig et al., 2014).

Conversely, offshore there is evidence for widespread synchronous subsidence since the Pliocene. In Gorontalo Bay, presumed Pliocene pinnacle reefs are found drowned in water depths of up to 2000 m (Jablonski et al., 2007; Pholbud et al., 2012; Hennig et al., 2014; Pezzati et al., 2014b, 2015).

The rapid extension and associated uplift onshore and subsidence offshore are linked to northward subduction hinge migration of the southward subducting Celebes Sea (Fig 16). Paleomagnetic data (Surmont et al., 1994) have been interpreted to indicate a 20°–25° clockwise rotation of the North Arm around a pole located at the eastern end of the North Arm, postdating the deposition of the Tinombo Formation, Ongka Volcanics, and Pani Volcanics (4.40 ± 0.20 Ma; Rudyawan et al., 2014). A complex pattern of seismicity below the North Arm (Gómez et al., 2000; Vigny et al., 2002; Beaudouin et al., 2003) and GPS data indicate that the North Arm is migrating northwards relative to Sundaland with a clockwise rotation of 3.4 ± 0.4°/Ma around a pole located at 2.1°N, 126.2°E (ENE of Manado) (Walpersdorf et al., 1998a) or ~2.6°/Ma around a pole at 2.4°N, 129.5°E (Socquet et al., 2006). Because of this clockwise motion, the convergence rates of the North Arm with the Celebes Sea vary from ~22 mm/a at the eastern Gorontalo station to ~44 mm/a at the Tomini station in the west (Socquet et al., 2006).

Subduction and strike-slip displacement on the Palu-Koro Fault have been considered to be mechanically linked (e.g. Silver et al., 1983b; Vigny et al., 2002; Govers and Wortel, 2005). GPS-defined slip rates on the Palu-Koro Fault range from 34 mm/a (Walpersdorf et al., 1998b) to 41–44 mm/a (Socquet et al., 2006). This slip rate is comparable with slip rate inferred from Holocene river offsets and restoration of the Pliocene rotation inferred from paleomagnetic data (Walpersdorf et al., 1998a; Bellier et al., 2006), suggesting that the instantaneous motions determined by GPS approximate the long term (geologic) rates. It is thus very likely that subduction roll-back in the Celebes Sea, uplift in North and Central Sulawesi, and subsidence in Gorontalo Bay, are still ongoing at the present day.

6. Conclusions

- The Cenozoic stratigraphy of NW Sulawesi is characterised by an Aquitanian and a Pliocene unconformity, related to (1) the collision of the Sula Spur and East Arm ophiolite with the North Arm and West Sulawesi, and (2) uplift associated with subsequent lithospheric extension respectively.
- The Malino Metamorphic Complex experienced lithospheric extension accommodated by widespread top-to-the-north mylonitic shear zones. Top-to-the-south extensional shearing is restricted to the southern margin of the MMC. This phase of extension occurred during the Early – Middle Miocene, as suggested by K–Ar and $^{40}Ar/^{39}Ar$ ages (van Leeuwen et al., 2007).

- Although the MMC experienced Early – Middle Miocene extension, there is no evidence that the MMC was exhumed during this time.
- The final phase of uplift was accommodated by brittle faulting identified on ASTER DEM imagery. These faults developed in Late Miocene to present day, according to crosscutting relations and age data of key geologic units.
- The absence of an unconformable contact between the MMC and the Ongka Volcanics does not support a pre-Pliocene age of exhumation. The presence of undeformed Pliocene granitoids intruding the MMC suggests the MMC was still at depth during their emplacement. Furthermore, the lack of metamorphic detritus in Pliocene-Pleistocene sedimentary formations, in stark contrast to abundant metamorphic float in Holocene alluvial deposits and present-day rivers suggests that exhumation of the MMC is very recent.
- There is widespread evidence of regional extension in North Sulawesi, linked to rotation of Sulawesi's North Arm which is likely associated with ongoing northward slab rollback of the southward subducting Celebes Sea since the Pliocene.

7. Acknowledgements

This work was made possible by the field assistance of Ramade Darmawan and our driver Agus. Boatmen and local guides Kisman, Baranti, Indra, Kamaludin, Abum and others provided help during the difficult work in river traverses of the Malino Metamorphic Complex. We thank Theo van Leeuwen, Giovanni Pezzati, Juliane Hennig, Jonathan Pownall and Mike Sandiford for useful discussions. Simon Suggate, Dominique Tanner and Benyamin Sapiie provided logistical and administrative support. This work was undertaken by the SE Asia Research Group at Royal Holloway, University of London which has been funded over many years by various consortia of oil companies. We thank Theo van Leeuwen and associate editor A.J. Barber for their constructive reviews.

8. References

Advokaat, E.L., Hall, R., White, L.T., Armstrong, R.A., Kohn, B.P., BouDagher-Fadel, M.K., 2014a. Neogene Extension and Exhumation in NW Sulawesi, AGU Fall Meeting Abstracts, pp. 4701.

Advokaat, E.L., van Hinsbergen, D.J.J., Kaymakcı, N., Vissers, R.L.M., Hendriks, B.W.H., 2014b. Late Cretaceous extension and Palaeogene rotation-related contraction in Central Anatolia recorded in the Ayhan-Büyükkışla basin. International Geology Review 56, 1813-1836.

Ahlburg, J., 1913. Versuch einer geologischen Darstellung der Insel Celebes. Neue Folge Band 12, heft 1 Jena, Gustav Fisher (also in Geologische und Palaontologische Abhandlungen. v.16/1, 172p 12.

Apandi, T., 1977. Geologic map of the Kotamobagu Quadrangle, North Sulawesi (Quadrangles 2316 - 2317) Scale 1: 250, 000. Geological Survey of Indonesia, Directorate of Mineral Resources, Geological Research and Development Centre, Bandung 20pp.

Bachri, S., Sukido, Ratman, N., 1994. Geology of the Tilamuta Sheet, Sulawesi (Quadrangles 2216 & 2217) Scale 1: 250, 000. Geological Survey of Indonesia, Directorate of Mineral Resources, Geological Research and Development Centre, Bandung 14pp.

Beaudouin, T., Bellier, O., Sebrier, M., 2003. Present-day stress and deformation field within the Sulawesi Island area (Indonesia): geodynamic implications. Bulletin de la Societe Geologique de France 174, 305-317.

Bellier, O., Sébrier, M., Seward, D., Beaudouin, T., Villeneuve, M., Putranto, E., 2006. Fission track and fault kinematics analyses for new insight into the Late Cenozoic tectonic regime changes in West-Central Sulawesi (Indonesia). Tectonophysics 413, 201-220.

Bergman, S.C., Coffield, D.Q., Talbot, J.P., Garrard, R.J., 1996. Tertiary Tectonic and Magmatic Evolution of Western Sulawesi and the Makassar Strait, Indonesia: Evidence for a Miocene Continent-Continent Collision. In: Hall, R., Blundell, D.J. (Eds.), Tectonic Evolution of SE Asia, Geological Society of London Special Publication, 106, 391-430.

BouDagher-Fadel, M.K., 2012. Biostratigraphic and geological significance of planktonic foraminifera, 22, Newnes.

Brouwer, H.A., 1934. Geologische onderzoekingen op het eiland Celebes. Verhandelingen Koninklijk Nederlands Geologisch en Mijnbouwkundig Genootschap, Geologische Serie V (10), 39-218.

Cavazza, W., Okay, A.I., Zattin, M., 2009. Rapid early-middle Miocene exhumation of the Kazdağ Massif (western Anatolia). International Journal of Earth Sciences 98, 1935-1947.

Chemenda, A.I., Mattauer, M., Bokun, A.N., 1996. Continental subduction and a mechanism for exhumation of high-pressure metamorphic rocks: new modelling and field data from Oman. Earth and Planetary Science Letters 143, 173-182.

de Roever, W.P., 1950. Preliminary notes on glaucophane-bearing and other crystalline schists from South East Celebes and on the origin of glaucophane bearing rocks. Proceedings Koninklijke Nederlandse Akademie van Wetenschappen, Amsterdam LIII-9 2-12.

Egeler, C.G., 1946. Contribution to the petrology of the metamorphic rocks of western Celebes. North Holland Publishing Corporation, Amsterdam 165pp.

Elburg, M., van Leeuwen, T., Foden, J., Muhardjo, 2003. Spatial and temporal isotopic domains of contrasting igneous suites in Western and Northern Sulawesi, Indonesia. Chemical Geology 199, 243-276.

Farr, T.G., Rosen, P.A., Caro, E., Crippen, R., Duren, R., Hensley, S., Kobrick, M., Paller, M., Rodriguez, E., Roth, L., 2007. The shuttle radar topography mission. Reviews of Geophysics 45.

Forster, M., Lister, G., 2009. Core-complex-related extension of the Aegean lithosphere initiated at the Eocene-Oligocene transition. Journal of Geophysical Research: Solid Earth (1978–2012) 114.

Gómez, J.M., Madariaga, R., Walpersdorf, A., Chalard, E., 2000. The 1996 Earthquakes in Sulawesi, Indonesia. Bulletin of the Seismological Society of America 90, 739-751.

Gradstein, F.M., Ogg, J.G., Schmitz, M., Ogg, G., 2012. The Geologic Time Scale 2012 2-Volume Set, 2, Elsevier.

GRDC, 1993. Penelitian sedimentologi Formasi Tinombo di daerah Kecamatan Tinombo, Kabupaten Donggala, Sulawesi Tengah. Annual Report GRDC 1992/1993 57–60.

Hall, R., 2009. The Eurasian SE Asian margin as a modern example of an accretionary orogen. Geological Society, London, Special Publications 318, 351-372.

Hall, R., 2011. Australia–SE Asia collision: plate tectonics and crustal flow. Geological Society, London, Special Publications 355, 75-109.

Hall, R., 2012. Late Jurassic–Cenozoic reconstructions of the Indonesian region and the Indian Ocean. Tectonophysics 570–571, 1-41.

Hall, R., Sevastjanova, I., 2012. Australian crust in Indonesia. Australian Journal of Earth Sciences 59, 827-844.

Hall, R., Wilson, M.E.J., 2000. Neogene sutures in eastern Indonesia. Journal of Asian Earth Sciences 18, 781-808.

Hamilton, W., 1979. Tectonics of the Indonesian region. U.S.G.S. Prof. Paper 1078 345pp.

Helmers, H., Maaskant, P., Hartel, T.H.D., 1990. Garnet peridotite and associated high-grade rocks from Sulawesi, Indonesia. Lithos 25, 171-188.

Helmers, H., Sopaheluwakan, J., Nila, E.S., Tjokrosapoetro, S., 1989. Blueschist evolution is Southeast Sulawesi, Indonesia. Netherlands Journal of Sea Research 24 (2), 373-381.

Hennig, J., Advokaat, E., Rudyawan, A., Hall, R., 2014. Large sediment accumulations and major subsidence offshore; rapid uplift on land: Consequences of extension of Gorontalo Bay and northern Sulawesi.

Hennig, J., Hall, R., Armstrong, R.A., 2016. U-Pb zircon geochronology of rocks from west Central Sulawesi, Indonesia: Extension-related metamorphism and magmatism during the early stages of mountain building. Gondwana Research 32 41-63.

Hennig, J., Hall, R., Watkinson, I.M., Forster, M., 2012. Timing and Mechanisms of Exhumation in West Central Sulawesi, Indonesia, AGU Fall Meeting Abstracts, pp. 2713.

Hinsbergen, D.J.J., Meulenkamp, J.E., 2006. Neogene supradetachment basin development on Crete (Greece) during exhumation of the South Aegean core complex. Basin Research 18, 103-124.

Jablonski, D., Priyono, R., Westlake, S., Larsen, O.A., 2007. Geology and exploration potential of the Gorontalo Basin, Central Indonesia - eastern extension of the North Makassar Basin? Indonesian Petroleum Association, Proceedings 31st Annual Convention 197-224.

Johnston, W.H., 1975. Bukal Prospect, Northern Sulawesi, Indonesia. Unpublished PT RioTinto Indonesia report No 16875.

Kadarusman, A., Brueckner, H.K., Yurimoto, H., Parkinson, C.D., Maruyama, S., 2001. Geochemistry and Sm-Nd dating of garnet peridotites from Central Sulawesi, and its implication to the Neogene collision complex in Eastern Indonesia, AGU Fall Meeting Abstracts, pp. 08.

Kadarusman, A., Miyashita, S., Maruyama, S., Parkinson, C.D., Ishikawa, A., 2004. Petrology, geochemistry and paleogeographic reconstruction of the East Sulawesi Ophiolite, Indonesia. Tectonophysics 392, 55-83.

Kadarusman, A., Parkinson, C.D., 2000. Petrology and PT evolution of garnet peridotites from central Sulawesi, Indonesia. Journal of Metamorphic Geology 18, 193-210.

Kadarusman, A., Sopaheluwakan, J., van Leeuwen, T., 2002. Eclogite, peridotite, granulite and associated high-grade rocks from Palu-Koro region, Central Sulawesi, Indonesia: An example for mantle and crust interactions in young orogenic belt, AGU Fall Meeting Abstracts, pp. 1230.

Kadarusman, A., van Leeuwen, T., Sopaheluwakan, J., 2011. Eclogite, peridotite, granulite and associated high-grade rocks from the Palu region, Central Sulawesi, Indonesia: an example of mantle and crust interaction in a young orogenic belt., Proc. Joint 36th HAGI and 40th IAGI Ann. Conv., Makassar, pp. 10.

Kadarusman, A., van Leeuwen, T.M., Soeria-Atmadja, R., 2005. Discovery of eclogite in the Palu Region, Central Sulawesi, and its implication for the tectonic evolution of Sulawesi. Special Edition Tertiary high-P metamorphism and associated ophiolite emplacement in Eastern Indonesia, Majalah Geologi Indonesia 20, 80-89.

Kavalieris, I., van Leeuwen, T.M., Wilson, M., 1992. Geological setting and styles of mineralization, north arm of Sulawesi, Indonesia. Journal of Southeast Asian Earth Sciences 7, 113-130.

Koperberg, M., 1929a. Bouwstoffen voor de geologie van de residentie Manado (deel I). Jaarboek van het Mijnwezen in Nederlandsch-Indië 57, 1-397.

Koperberg, M., 1929b. Bouwstoffen voor de geologie van de residentie Manado (deel II en III). Jaarboek van het Mijnwezen in Nederlandsch-Indië 57, 1-446.

Kündig, E., 1956. Geology and ophiolite problems of East Celebes. Verhandelingen Koninklijk Nederlands Geologisch en Mijnbouwkundig Genootschap, Geologische Serie 16, 210-235.

Lister, G., Forster, M., 2009. Tectonic mode switches and the nature of orogenesis. Lithos 113, 274-291.

Maulana, A., 2013. A Petrochemical study of the Late Cenozoic Granitic Rock from Sulawesi Indonesia, Kyushu University, Fukuoka, 167 pp.

Maulana, A., Imai, A., Van Leeuwen, T., Watanabe, K., Yonezu, K., Nakano, T., Boyce, A., Page, L., Schersten, A., 2016. Origin and geodynamic setting of Late Cenozoic granitoids in Sulawesi, Indonesia. Journal of Asian Earth Sciences 124, 102-125.

Molengraaff, G.A.F., 1902. Über die Geologie der Umgebend von Sumalatta auf Nord-Celebes und über die dort vorkommenden goldführenden Erzgänge. Zeitschrift für praktische Geologie 10, 249-257.

Parkinson, C., 1998a. Emplacement of the East Sulawesi Ophiolite: evidence from subophiolite metamorphic rocks. Journal of Asian Earth Sciences 16, 13-28.

Parkinson, C., 1998b. An outline of the petrology, structure and age of the Pompangeo Schist Complex of central Sulawesi, Indonesia. Island Arc 7, 231-245.

Pezzati, G., Hall, R., Burgess, P., Perez-Gussinye, M., 2014a. Pliocene Core Complex Exhumation on Land and Rapid Subsidence in Gorontalo Bay, Sulawesi (Indonesia), AGU Fall Meeting Abstracts, pp. 4702.

Pezzati, G., Hall, R., Burgess, P., Perez-Gussinye, M., 2014b. The Poso Basin in Gorontalo Bay, Sulawesi: extension related to core complex formation on land, Indonesian Petroleum Association, Proceedings 38th Annual Convention, pp. IPA14-G-297.

Pezzati, G., Hennig, J., Advokaat, E., Hall, R., Burgess, P., Perez-Gussinye, M., 2015. Subsidence in Gorontalo Bay, Sulawesi (Indonesia) and metamorphic core complex exhumation on land, EGU General Assembly Conference Abstracts, pp. 7476.

Pholbud, P., Hall, R., Advokaat, E.L., Burgess, P., Rudyawan, A., 2012. A new interpretation of Gorontalo Bay, Indonesia, Indonesian Petroleum Association, Proceedings 36th Annual Convention, pp. IPA12-G-029.

Platt, J.P., Vissers, R.L.M., 1989. Extensional collapse of thickened continental lithosphere: a working hypothesis for the Alboran Sea and Gibraltar Arc. Geology 17, 540-543.

Polvé, M., Maury, R.C., Bellon, H., Rangin, C., Priadi, B., Yuwono, S., Joron, J.L., Atmadja, R.S., 1997. Magmatic evolution of Sulawesi (Indonesia): Constraints on the Cenozoic geodynamic history of the Sundaland active margin. Tectonophysics 272, 69-92.

Pownall, J.M., Hall, R., Armstrong, R.A., Forster, M.A., 2014. Earth's youngest known ultrahigh-temperature granulites discovered on Seram, eastern Indonesia. Geology 42, 279-282.

Pownall, J.M., Hall, R., Watkinson, I.M., 2013. Extreme extension across Seram and Ambon, eastern Indonesia: evidence for Banda slab rollback. Solid Earth 4, 277-314.

Priadi, B., Polvé, M., Maury, R., Soeria-Atmadja, R., Bellon, H., 1993. Geodynamic implications of Neogene potassic calc alkaline magmatism in central of Sulawesi: geochemical and isotopic constraints. In: Proceedings of the 22nd Annual Convention of the Indonesian Association of Geologists (IAGI) 1 59-81.

Rangin, C., Maury, R.C., Bellon, H., Cotten, J., Polve, M., Priadi, B., Soeria-Atmadja, R., Joron, J.-L., 1997. Eocene to Miocene back-arc basin basalts and associated island arc tholeiites from northern Sulawesi (Indonesia): implications for the geodynamic evolution of the Celebes basin.

Ratman, N., 1976. Geological Map of the Tolitoli Quadrangle, North Sulawesi (Quadrangle 2016 - 2116 - 2117) - Scale 1:250, 000. Geological Survey of Indonesia, Directorate of Mineral Resources, Geological Research and Development Centre, Bandung.

Rudyawan, A., 2016. Neogene structures and exhumation in central North Sulawesi. unpublished PhD thesis Thesis, University of London.

Rudyawan, A., Hall, R., and White, L., 2014. Neogene extension of the central north Arm of Sulawesi, Indonesia. In AGU Fall Meeting December.

Rutten, L.M.R., 1927. Voordrachten over de geologie van Nederlandsch Oost-Indië. Wolters, Groningen 839pp.

Sarasin, P., Sarasin, S., 1901. Entwurf einer geografisch - geologischen beschreibung der Insel Celebes. Wiesbaden, Deutschland.

Schubert, R.J., 1913. Beitrag zur fossilen Foraminiferenfauna von Celebes. Jahrbuch des kaiserlich-koniglichen geologischen Reichanstalt 63, 127-150.

Searle, M.P., Szulc, A.G., 2005. Channel flow and ductile extrusion of the high Himalayan slab-the Kangchenjunga–Darjeeling profile, Sikkim Himalaya☆. Journal of Asian Earth Sciences 25, 173-185.

Silver, E.A., McCaffrey, R., Smith, R.B., 1983. Collision, rotation, and the initiation of subduction in the evolution of Sulawesi, Indonesia. Journal of Geophysical Research 88, 9407-9418.

Simandjuntak, T.O., 1986. Sedimentology and tectonics of the collision complex in the East Arm of Sulawesi, Indonesia. Ph.D. Thesis, University of London (Unpublished) 374pp.

Socquet, A., Simons, W., Vigny, C., McCaffrey, R., Subarya, C., Sarsito, D., Ambrosius, B., Spakman, W., 2006. Microblock rotations and fault coupling in SE Asia triple junction (Sulawesi, Indonesia) from GPS and earthquake slip vector data. Journal of Geophysical Research: Solid Earth (1978–2012) 111.

Spakman, W., Hall, R., 2010. Surface deformation and slab–mantle interaction during Banda arc subduction rollback. Nature Geoscience 3, 562-566.

Spencer, J.E., 2010. Structural analysis of three extensional detachment faults with data from the 2000 Space-Shuttle Radar Topography Mission. GSA Today 20, 4-10.

Spencer, J.E., 2011. Gently dipping normal faults identified with Space Shuttle radar topography data in central Sulawesi, Indonesia, and some implications for fault mechanics. Earth and Planetary Science Letters 308, 267-276.

Surmont, J., Laj, C., Kissel, C., Rangin, C., Bellon, H., Priadi, B., 1994. New paleomagnetic constraints on the Cenozoic tectonic evolution of the North Arm of Sulawesi, Indonesia. Earth and Planetary Science Letters 121, 629-638.

Taylor, D., Van Leeuwen, T., 1980. Porphyry-type deposits in Southeast Asia. Mining Geology, Speeial 15 95-116.

Trail, D.S., Bird, M.C., Obiab, R.C., Parwoto, Pertzel, B.A., 1972. Progress report Block 2, Sulawesi Utara, Idonesia. PT Tropical Endeavour Indonesia (Unpublished).

Trail, D.S., John, T.V., Bird, M.C., Obial, R.C., Pertzel, D.A., Abiog, D.B., Parwoto, Subiago, 1974. The general geological survey of block II, Sulawesi Utara, Indonesia. PT Tropical Endeavour Indonesia (Unpublished).

van Leeuwen, T., Allen, C.M., Elburg, M., Massonne, H.-J., Palin, J.M., Hennig, J., 2016. The Palu Metamorphic Complex, NW Sulawesi, Indonesia: Origin and evolution of a young metamorphic terrane with links to Gondwana and Sundaland. Journal of Asian Earth Sciences 115 133-152.

van Leeuwen, T., Allen, C.M., Kadarusman, A., Elburg, M., Michael Palin, J., 2007. Petrologic, isotopic, and radiometric age constraints on the origin and tectonic history of the Malino Metamorphic Complex, NW Sulawesi, Indonesia. Journal of Asian Earth Sciences 29, 751-777.

van Leeuwen, T., Muhardjo, 2005. Stratigraphy and tectonic setting of the Cretaceous and Paleogene volcanic-sedimentary successions in northwest Sulawesi, Indonesia: implications for the Cenozoic evolution of Western and Northern Sulawesi. Journal of Asian Earth Sciences 25 481-511.

van Leeuwen, T.M., Susanto, E.S., Maryanto, S., Hadiwisastra, S., 2010. Tectonostratigraphic evolution of Cenozoic marginal basin and continental margin successions in the Bone Mountains, Southwest Sulawesi, Indonesia. Journal of Asian Earth Sciences 38, 233-254.

van Leeuwen, T.M., Taylor, R., Coote, A., Longstaffe, F.J., 1994. Porphyry molybendum mineralization in a continental collision setting at Malala, northwest Sulawesi, Indonesia. Journal of Geochemical Exploration. Special Issue - Mineral deposits of Indonesia - Discoveries of the past 25 years. 50, 279-315.

Vigny, C., Perfettini, H., Walpersdorf, A., Lemoine, A., Simons, W., van Loon, D., Ambrosius, B., Stevens, C., McCaffrey, R., Morgan, P., 2002. Migration of seismicity and earthquake interactions monitored by GPS in SE Asia triple junction: Sulawesi, Indonesia. Journal of Geophysical Research: Solid Earth (1978–2012) 107, ETG 7-1-ETG 7-11.

Villeneuve, M., Gunawan, W., Cornee, J.J., Vidal, O., 2002. Geology of the central Sulawesi belt (eastern indonesia): constraints for geodynamic models. International Journal of Earth Sciences 91 524-537.

Walpersdorf, A., Rangin, C., Vigny, C., 1998a. GPS compared to long-term geologic motion of the north arm of Sulawesi. Earth and Planetary Science Letters 159, 47-55.

Walpersdorf, A., Vigny, C., Subarya, C., Manurung, P., 1998b. Monitoring of the Palu-Koro Fault (Sulawesi) by GPS. Geophysical Research Letters 25, 2313-2316.

Watkinson, I.M., 2011. Ductile flow in the metamorphic rocks of central Sulawesi. Geological Society, London, Special Publications 355, 157-176.

Watkinson, I.M., Hall, R., Hennig, J., Forster, M., 2012. Extension Within The Australia-Eurasia Collision: The Metamorphic Rocks Of Central Sulawesi, Indonesia, AGU Fall Meeting Abstracts, pp. 2715.

White, L.T., Graham, I., Tanner, D., Hall, R., Armstrong, R.A., Yaxley, G., Barron, L., Spencer, L., van Leeuwen, T.M., 2016. The provenance of Borneo's enigmatic alluvial diamonds: A case study from Cempaka, SE Kalimantan. Gondwana Research 38 251-272.

White, L.T., Hall, R., Armstrong, R.A., Barber, A.J., Boudagher-Fadel, M., Baxter, A., Wakita, K., Manning, C., 2017. The geological history of the Latimojong Mountains and Toraja region of Sulawesi. Journal of Asian Earth Sciences.

Yamaguchi, Y., Kahle, A.B., Tsu, H., Kawakami, T., Pniel, M., 1998. Overview of advanced spaceborne thermal emission and reflection radiometer (ASTER). Geoscience and Remote Sensing, IEEE Transactions on 36, 1062-1071.

9. Figure captions

1. A) Paleozoic to Cenozoic accretion of Gondwanan blocks in SE Asia, modified from Hall and Sevastjanova (2012). B) Summary of the geology of Sulawesi, modified from Hall and Wilson (2000), Kadarusman et al. (2004), Watkinson (2011) and White et al. (2017). Heavy dashed line indicates the approximate maximum extent of continental crust of the Sula Spur. In Central Sulawesi, this coincides with the position of the Early Miocene suture. In the South Arm, the position of the suture is uncertain. The North Arm is partly underlain by

continental crust of the Sula Spur MMC = Malino Metamorphic Complex; PMC = Palu Metamorphic Complex; TM = Tokorondo Mountains; PM = Pompangeo Mountains; LC = Latimojong Complex.

2. Geologic map of the study area, with SRTM shaded relief basemap. Outlines are based on new geological field mapping (this study), DEM fault interpretation (Pholbud et al., 2012; this study), and previously published maps (Koperberg, 1929c; Brouwer, 1934; Ratman, 1976; Bachri et al., 1994; van Leeuwen et al., 1994). Black boxes indicate location of detailed sketch maps, accompanying numbers indicate figure numbers. Line X-Y indicates location of regional cross section (Fig. 17).

3. Chronostratigraphic diagram for NW Sulawesi. Left hand diagram shows schematic extent of formations in space and time. Right hand diagram shows fossil age ranges of samples collected in this study, see Fig. 2 for location. Light grey shaded area indicate age range estimates for Papayato Volcanics and Tinombo Formation (van Leeuwen and Muhardjo, 2005), dark grey shaded boxes indicate common age of samples from this study. Timescale based on Gradstein et al. (2012). Paleontological ages after BouDagher-Fadel (2012).

4. Sungai Silondou (120.7880°E, 0.7563°E): A) Outcrop photo, showing greenschist and quartz bands. The quartz bands show stretching lineations, which are subsequently folded. B) Thin section micrograph (under plain polarised light), parallel to stretching lineation, perpendicular to foliation, showing chlorite mica fish and a pervasive C'-fabric with a top-to-the-north-sense of shear.

5. Sungai Ngesgani: A) Detailed sketch map. See Fig. 2 for location. B) Profile, modified from Hennig et al. (2014). Black semicircles on the faults indicate downthrown side of the faults. Legend also applies for Fig. 7 and 10.

6. S. Ngesgani: A; B) Greenschist juxtaposed against the Tinombo Formation by brittle faults (120.9057°E, 0.7905°N), C) Greenschist crosscut by deformed quartz veins (120.9184°E, 0.6579°N), D) Quartz veins in greenschist, deformed by sheath folding (120.9184°E, 0.6579°N), E; F) Outcrop of quartz-muscovite gneiss with localised folding (120.9187°E, 0.7704°N).

7. Jalan Kotaraya-Tolitoli: A) Sketch map. See Fig. 2 for location. B) Cross section through western part of MMC. Colours and symbols as in Fig. 5.

8. Jalan Kotaraya: A) Intensely weathered, steeply dipping mica schists (120.6636°E, 0.6642°N). B) Close up of (A), showing fault plane with slickenlines, C) Undeformed diorite faulted against muscovite gneiss (120.6646°E, 0.6635°N). D) Close up of (C), showing

anastomosing shear zones. E; F) Float boulder showing intrusive relation between diorite and muscovite gneiss; note the injection of the diorite into the gneiss (120.6646°E, 0.6635°N).

9. SW boundary of the MMC. A) Quartz σ-clast in greenschist (120.5725°E, 0.5379°N). B) Micrograph of epidote-chlorite-quartz greenschist, with crosscutting calcite vein. Quartz grains show imbricated subgrain rotation. Orientation parallel to stretching lineation, perpendicular to foliation (120.5725°E, 0.5379°N). C) Epidote-chlorite-garnet schist. Garnet σ-clast surrounded by chlorite, indicating top-to-the-north sense of shear (120.5769°E, 0.5402°N). D) Low angle fault 120.5783°E, 0.5464°N); E) macroscopic c-fabric shears, indicating a dextral sense of motion 120.6736°E, 0.5534°N). F) Chlorite-epidote schist with NE-SW-trending subvertical foliation and SW-plunging stretching lineations (120.7185°E, 0.5772°N).

10. Sungai Duyun: A) Detailed sketch map. See Fig. 2 for location. B) Profile. Colours as in Figure 5. Sungai Sinobulu: C) Detailed sketch map. See Fig. 2 for location. D) Profile. Colours as in Fig. 5.

11. Sungai Sinobulu. Left column: field photographs; right column: corresponding thin section micrographs under cross polarised light, oriented parallel to stretching lineation, perpendicular to foliation. A) Chlorite-epidote-plagioclase greenschist with thin quartz bands (121.0832°E, 0.5704°N). B) Upper part shows quartz band with quartz grains experiencing imbricated subgrain rotation, lower part shows chlorite, epidote and plagioclase. C) Outcrop of garnet schist showing well developed foliation and weak stretching lineations (121.0832°E, 0.5713°N). D) Garnet porphyroblast with δ-tails of quartz. E) Monoclinally folded quartz muscovite crosscut by folded quartz vein (120.0830°E, 0.5740°N). F) Muscovite mica fish bordered by C’-fabric shear bands defined by muscovite and recrystallized quartz 121.0823°E, 0.5748°N.

12. Sungai Siguru: A) Detailed sketch map. See Fig. 2 for location; B) Profile, modified from Hennig et al. (2014).

13. Sungai Siguru. See Fig. 15 for location. Modified from Hennig et al. (2014). A) Wide fault gouge zone (>100 m) between metamorphic rocks of the Malino Metamorphic Complex and overlying Papayato Volcanics with B) Foliated fragments (c. 30 cm in length) and C) Angular volcanic fragments (121.1287°E, 0.5381°N). D) Quartz-muscovite schist showing an undulating foliation and stretching lineations (121.1340°E, 05568°N). E) Thin section micrograph (under cross polarised light) parallel to stretching lineation, perpendicular to foliation, showing muscovite mica fish bordered by C’-fabrics indicating a top-to-the-NE sense of shear (121.1340°E, 0.5568°N).

14. Tolitoli region: A) Deformed shales from the Tinombo Formation in southern Tolitoli (120.7820°E, 0.7874°N). B) Sequence of basaltic pillow lavas and intercalations of red calcareous mudstone (120.8586°E, 0.9118°N). C) Complex intrusive contact relations between slates of Tinombo Formation and granodiorite of Dondo Suite, D; E) Close up of contact, showing coarse grained granodiorite (120.6243°E, 0.9052°N).
15. A) Outcrops exposing a fault zone in Sungai Batu Bota, a tributary of Sungai Lembah Fitra; B) Micrograph of brecciated rocks in the fault zone of Sungai Batu Bota (120.9080°E, 1.0040°N). C; D) Thrust faults in an outcrop along the north coast exposing a turbiditic sequence of the Tinombo Fomation (121.0218°E, 1.3265°N).
16. Interpreted faults from ASTER DEM, and principal structural features of northern Sulawesi, modified from Pholbud et al. (2012)
17. Regional cross section. See Fig. 2 for location.

10. Tables

1. Microfaunal assemblages for samples of sedimentary rocks from NW Sulawesi. Age based on first appearance, planktonic foraminiferal zones and letter stages after BouDagher-Fadel (2008).

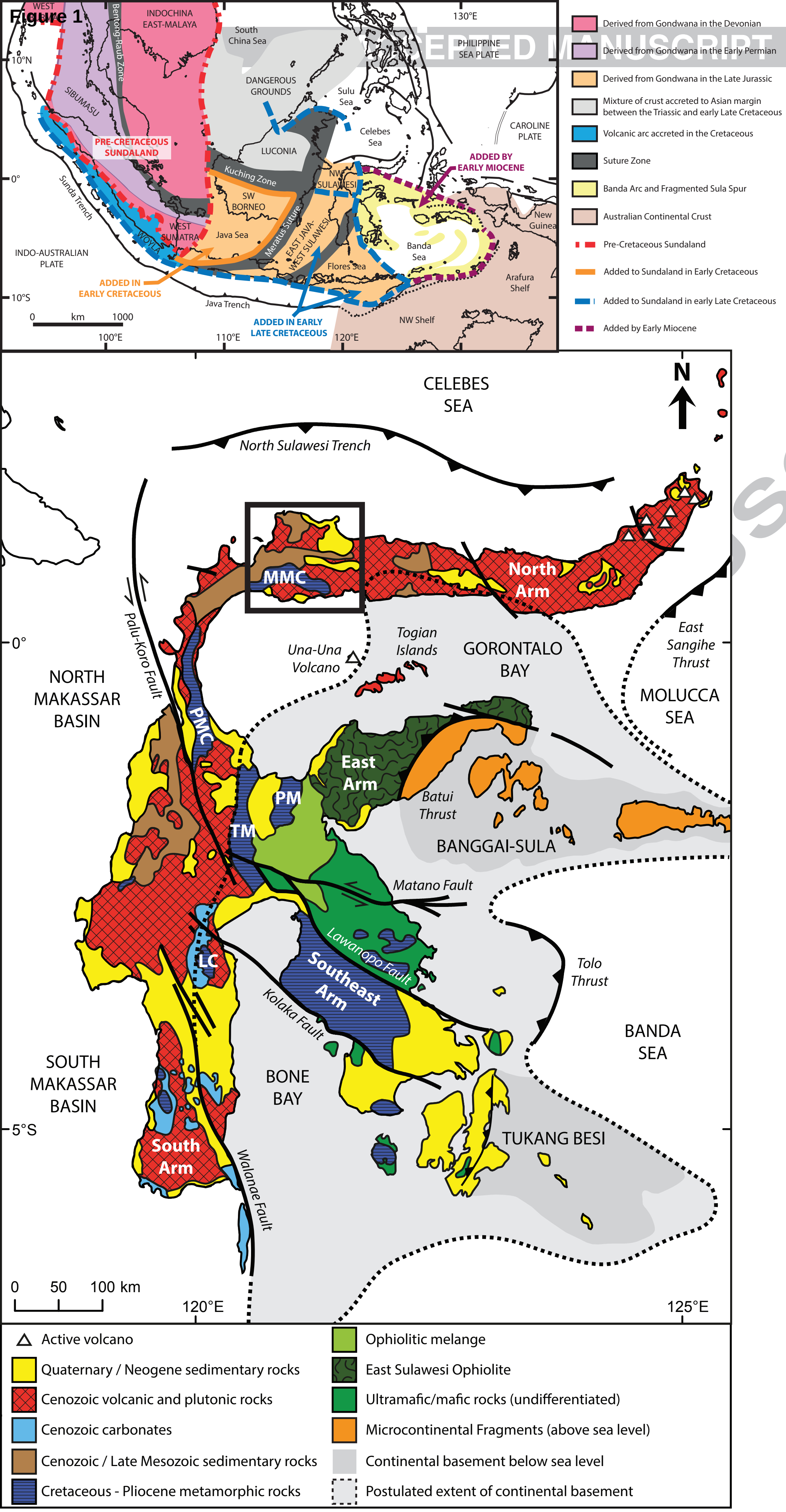

Figure 1
WEST
INDOCHINA
EAST-MALAYA
Bentong-Raub Zone
South China Sea
SIBUMASU
DANGEROUS GROUNDS
PHILIPPINE SEA PLATE
Sulu Sea
Celebes Sea
CAROLINE PLATE
LUCONIA
PRE-CRETACEOUS SUNDALAND
Kuching Zone
NW SULAWESI
ADDED BY EARLY MIOCENE
SW BORNEO
Meratus Suture
EAST JAVA-WEST SULAWESI
WEST SUMATRA
WOYLA
Java Sea
Sunda Trench
Banda Sea
New Guinea
Flores Sea
Arafura Shelf
INDO-AUSTRALIAN PLATE
ADDED IN EARLY CRETACEOUS
Java Trench
ADDED IN EARLY LATE CRETACEOUS
NW Shelf
0 km 1000
10°N
0°
10°S
100°E
110°E
120°E
130°E
Derived from Gondwana in the Devonian
Derived from Gondwana in the Early Permian
Derived from Gondwana in the Late Jurassic
Mixture of crust accreted to Asian margin between the Triassic and early Late Cretaceous
Volcanic arc accreted in the Cretaceous
Suture Zone
Banda Arc and Fragmented Sula Spur
Australian Continental Crust
Pre-Cretaceous Sundaland
Added to Sundaland in Early Cretaceous
Added to Sundaland in early Late Cretaceous
Added by Early Miocene
CELEBES SEA
N
North Sulawesi Trench
MMC
North Arm
Palu-Koro Fault
0°
Una-Una Volcano
Togian Islands
GORONTALO BAY
East Sangihe Thrust
NORTH MAKASSAR BASIN
MOLUCCA SEA
PMC
East Arm
PM
Batui Thrust
TM
BANGGAI-SULA
Matano Fault
Lawanopo Fault
LC
Tolo Thrust
Southeast Arm
Kolaka Fault
BANDA SEA
SOUTH MAKASSAR BASIN
BONE BAY
5°S
TUKANG BESI
South Arm
Walanae Fault
0 50 100 km
120°E
125°E
Active volcano
Quaternary / Neogene sedimentary rocks
Cenozoic volcanic and plutonic rocks
Cenozoic carbonates
Cenozoic / Late Mesozoic sedimentary rocks
Cretaceous - Pliocene metamorphic rocks
Ophiolitic melange
East Sulawesi Ophiolite
Ultramafic/mafic rocks (undifferentiated)
Microcontinental Fragments (above sea level)
Continental basement below sea level
Postulated extent of continental basement

Figure 1

Figure 2

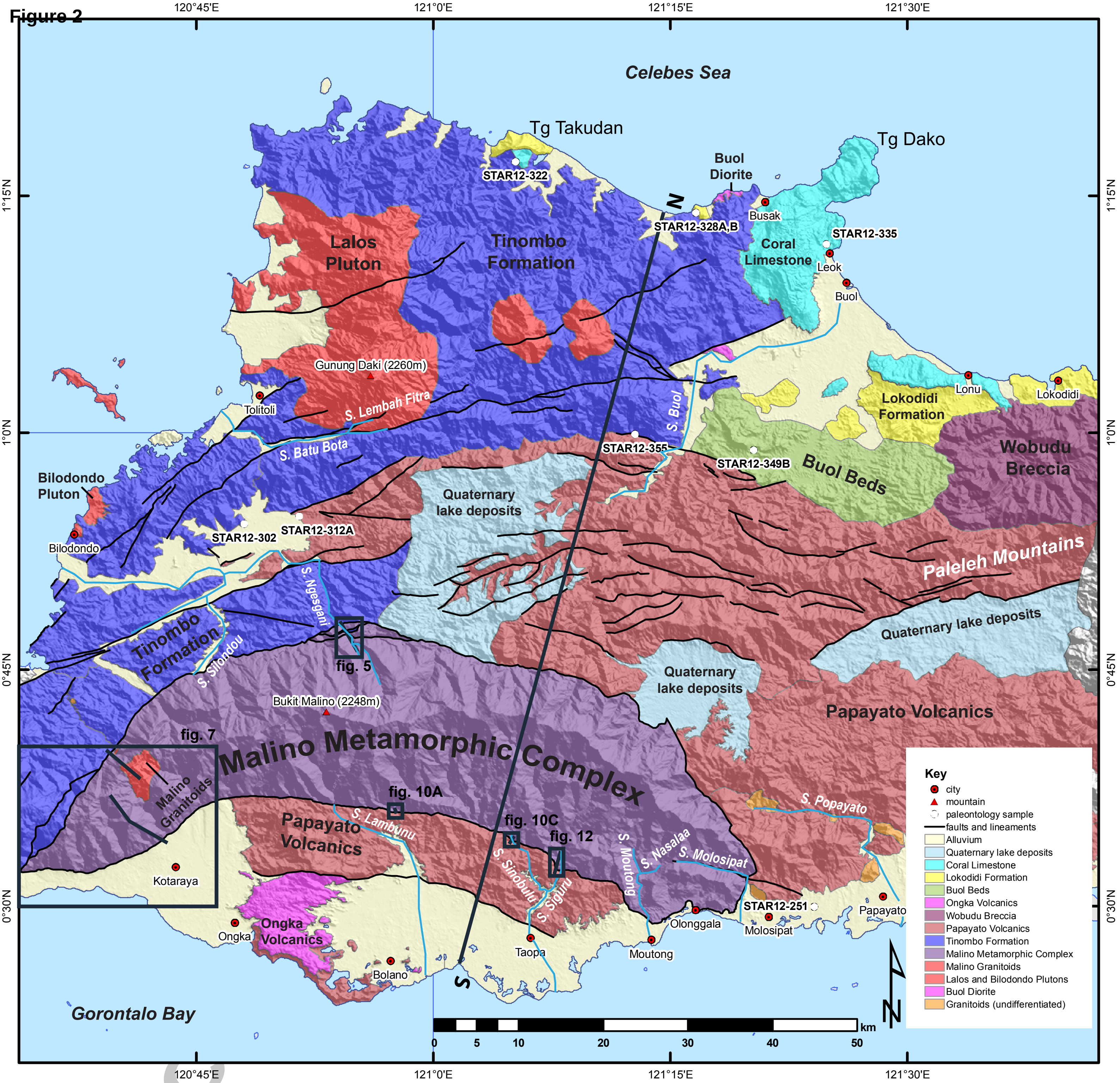

Figure 2

Figure 3

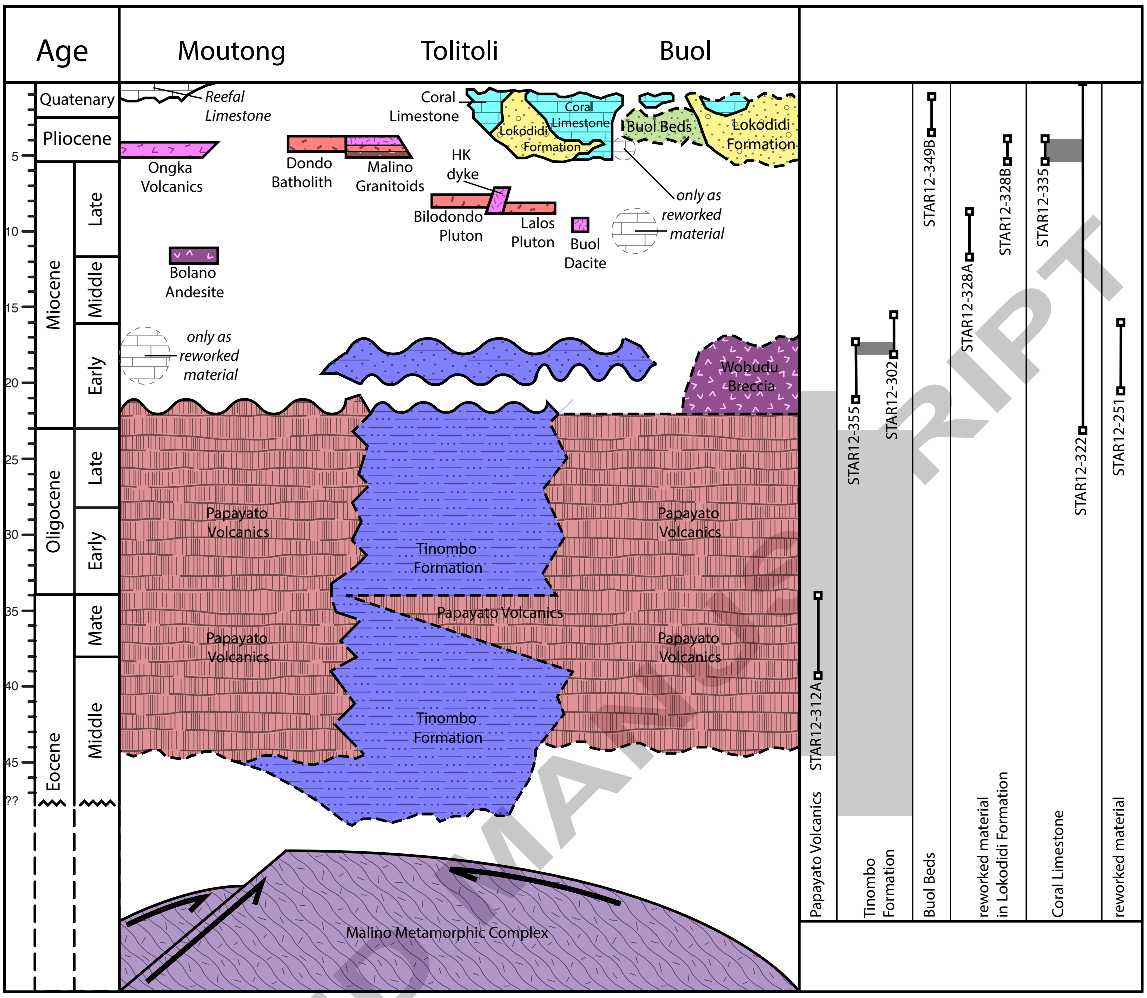

Figure 3.

Figure 4

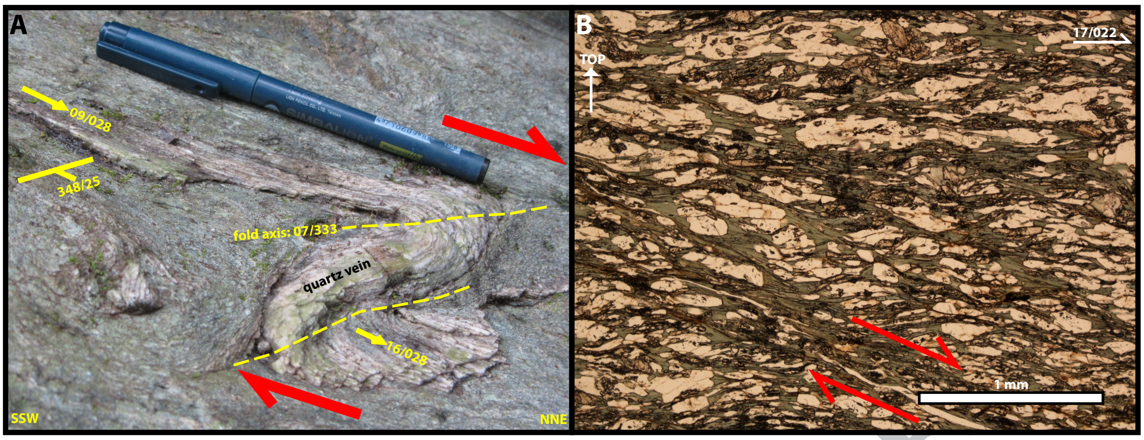

Figure 4

Figure 5

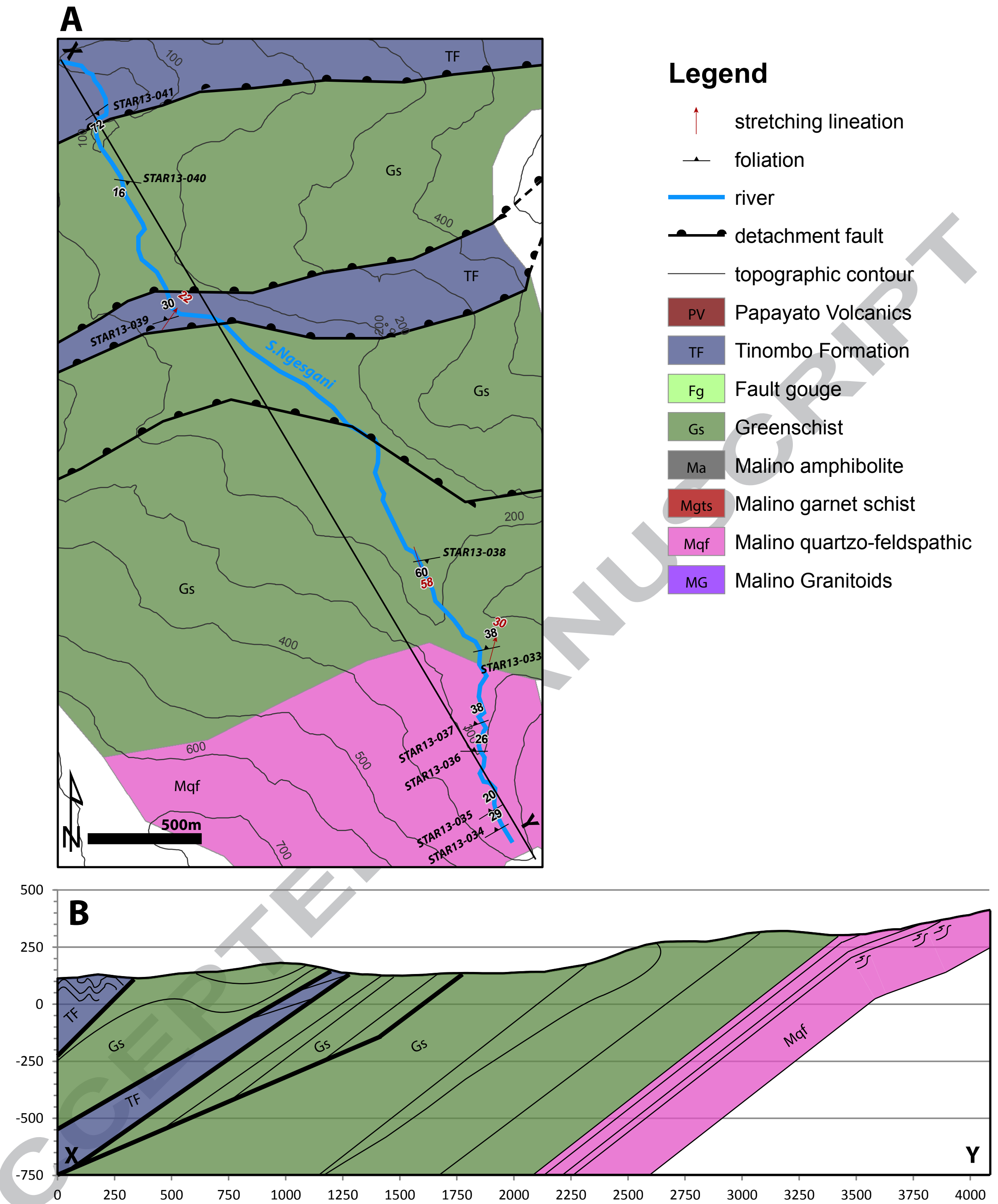

Figure 5

Figure 6

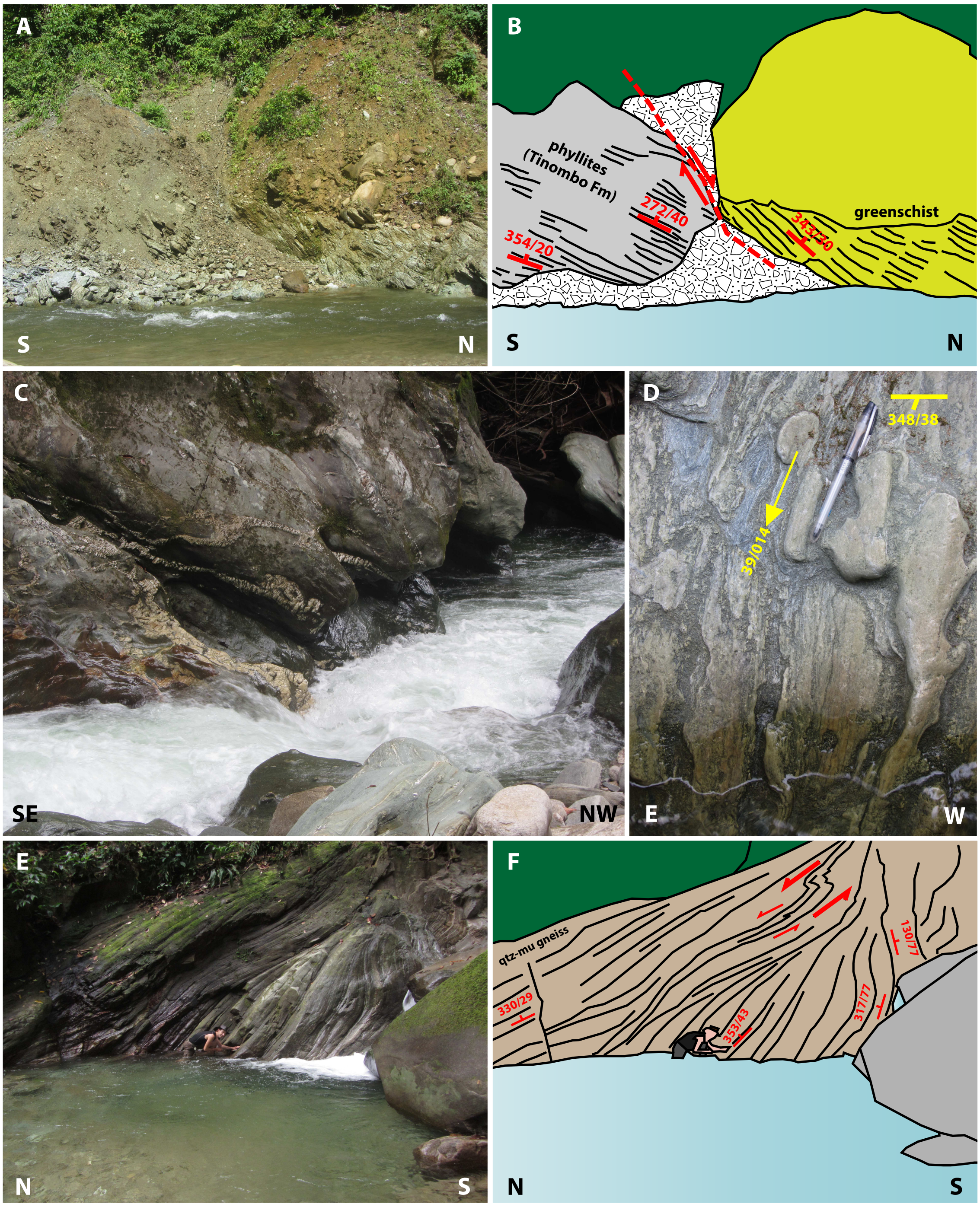

Figure 6

Figure 7

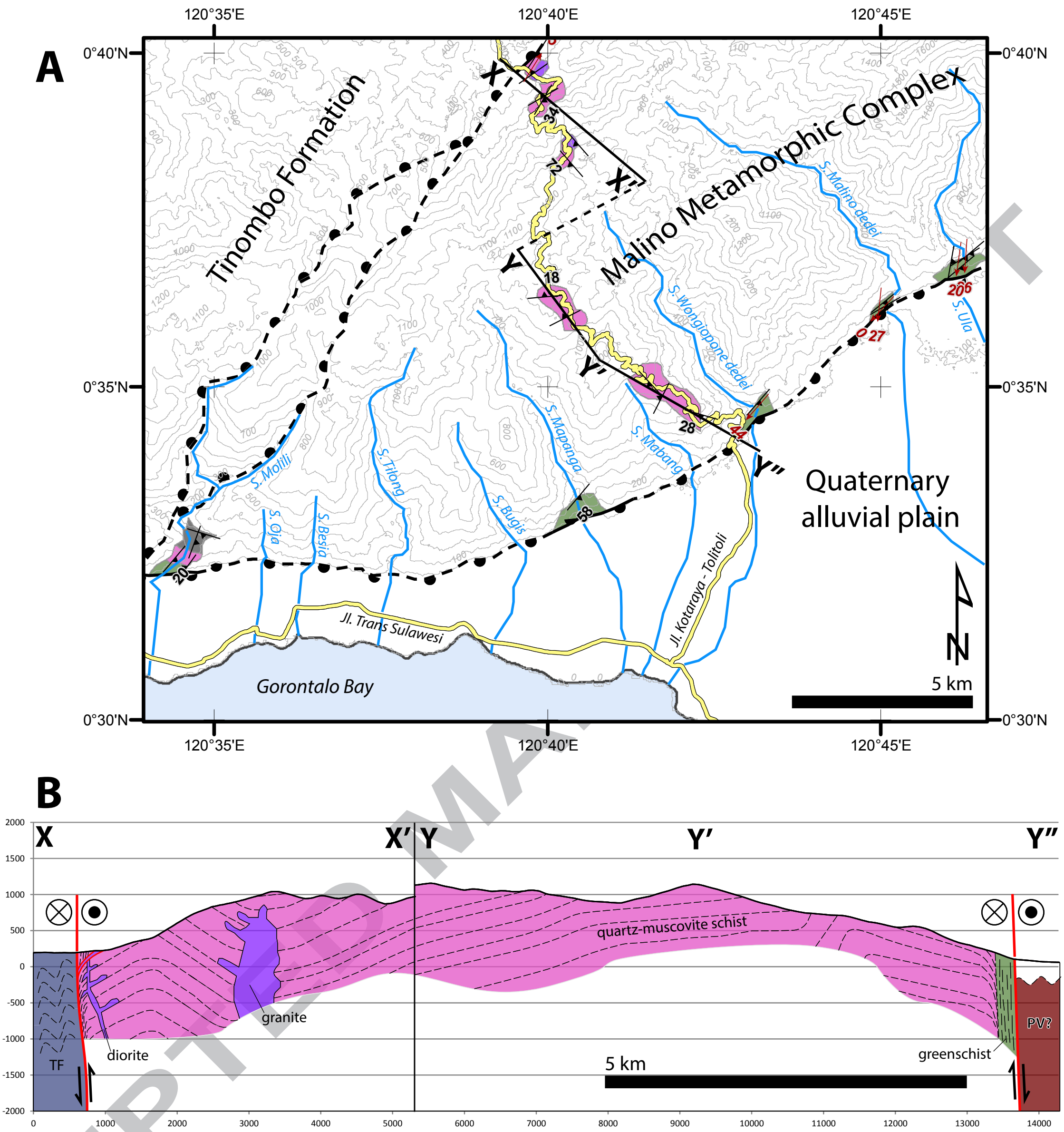

Figure 7

Figure 8

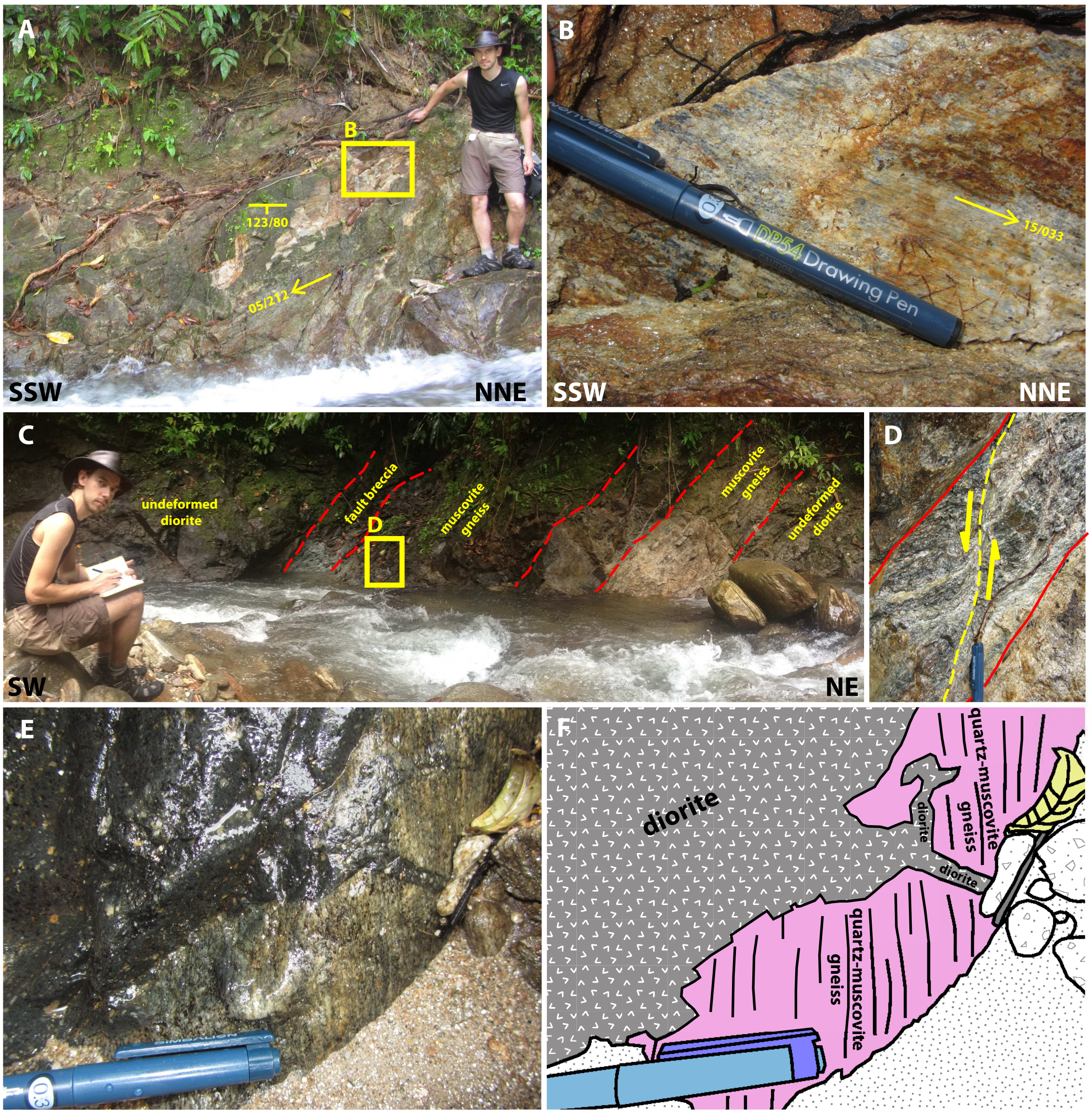

Figure 8

Figure 9

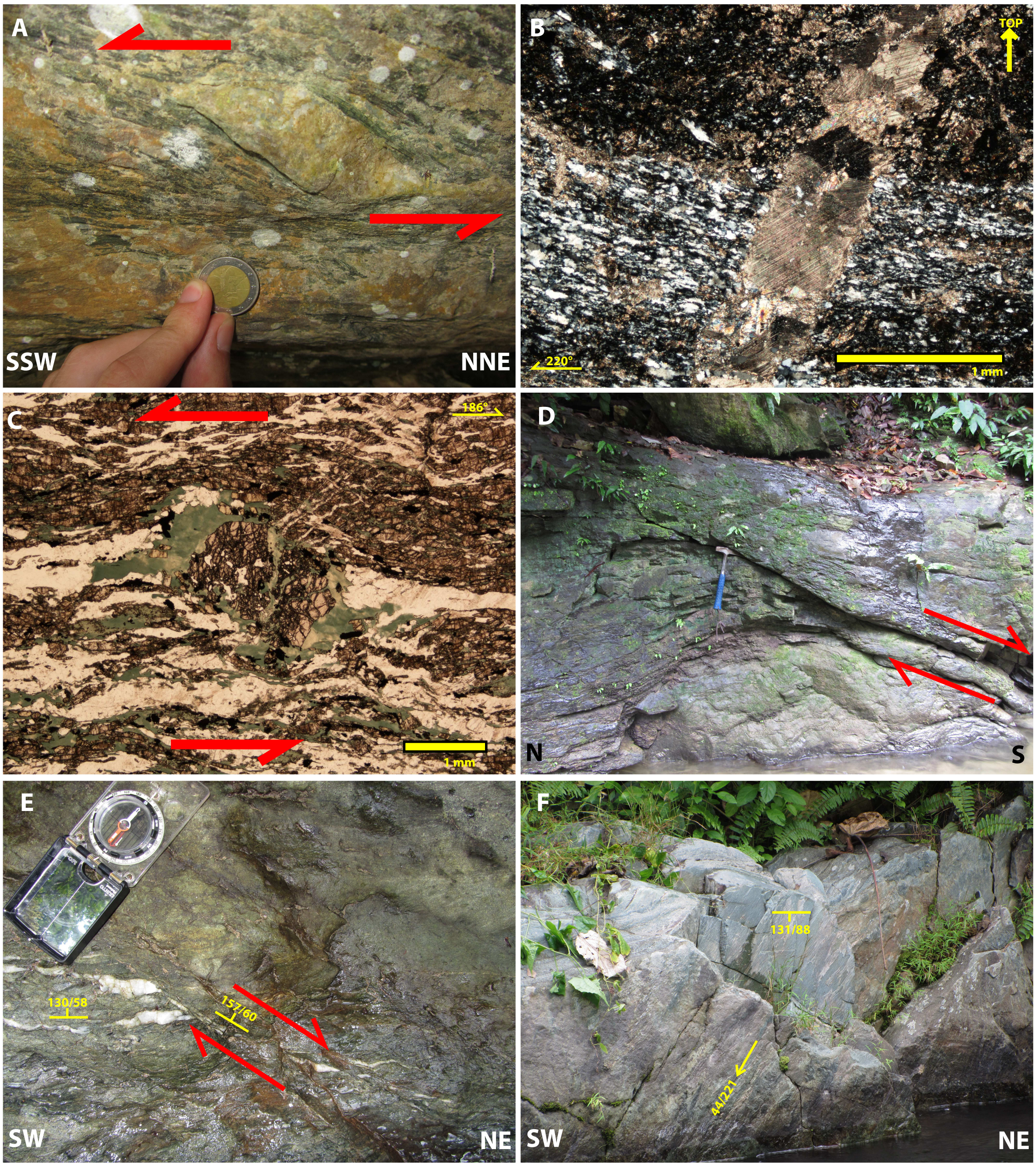

Figure 9

Figure 10

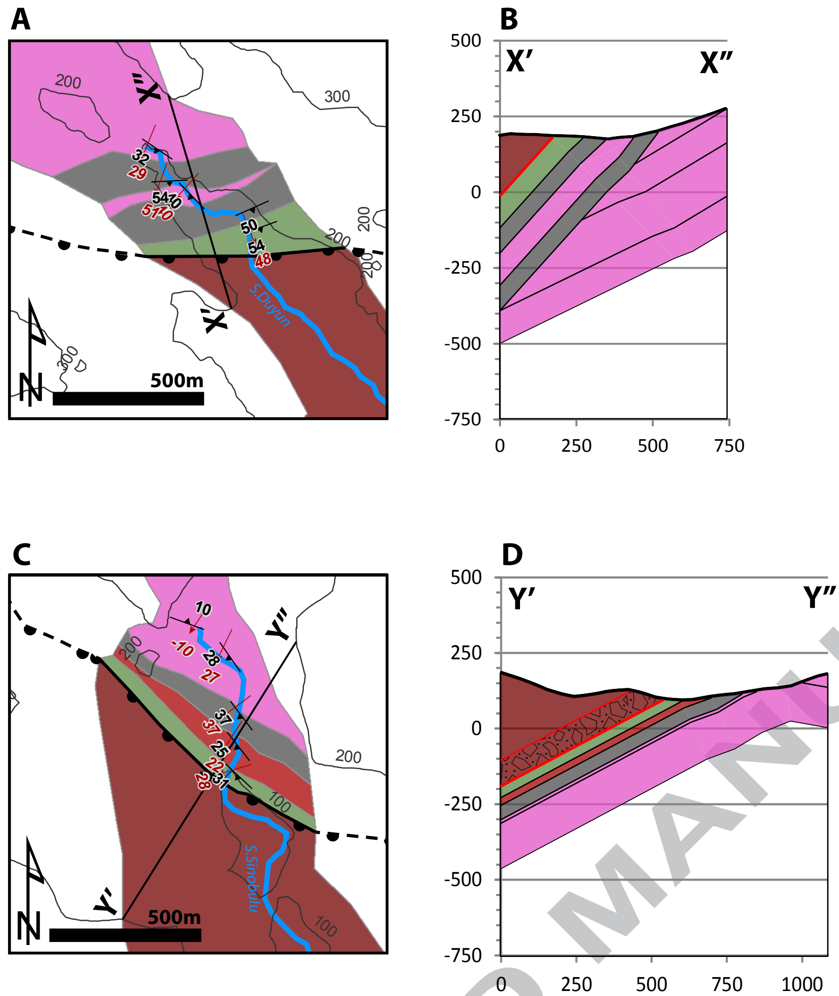

Figure 10

Figure 11

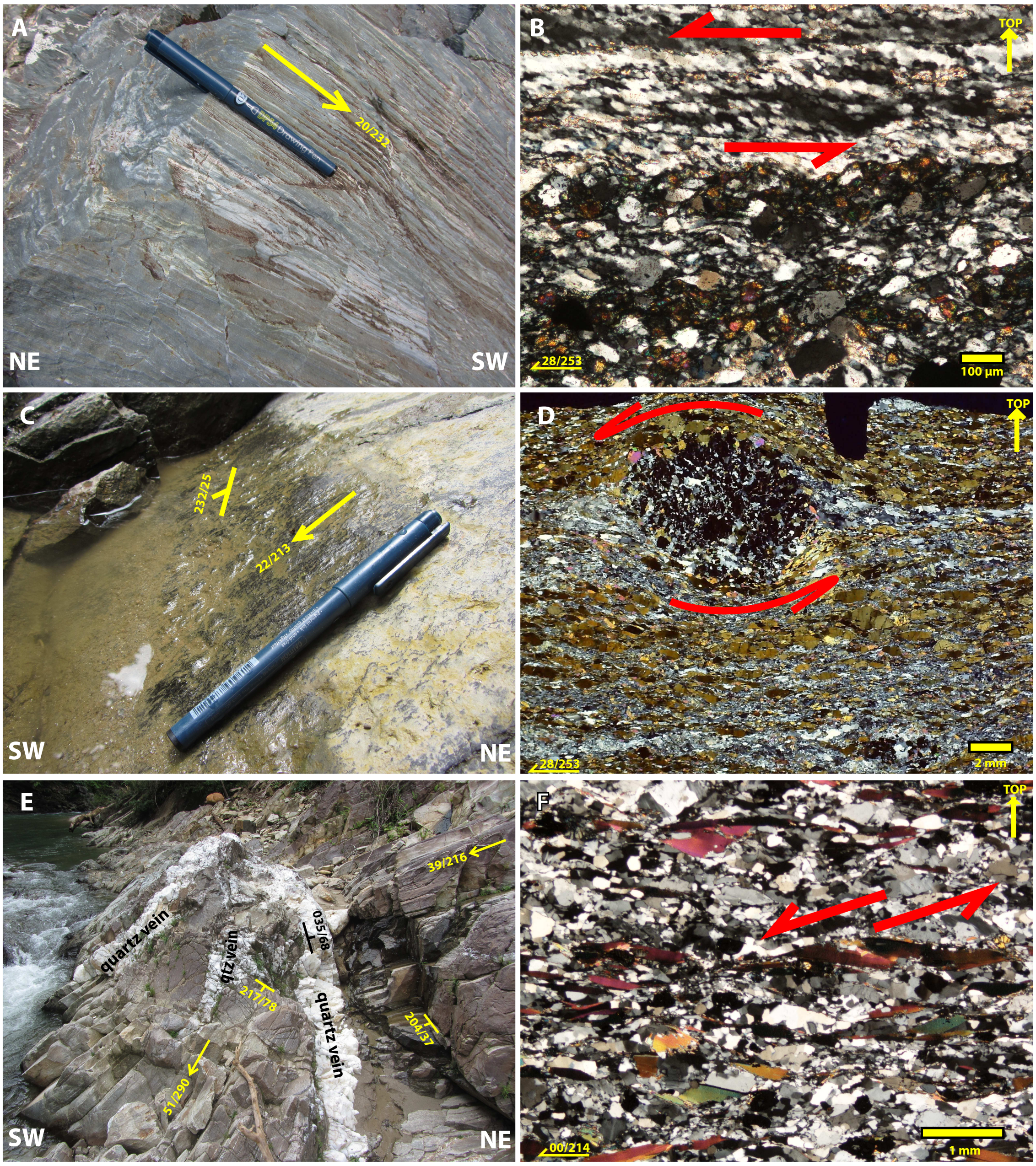

Figure 11

Figure 12

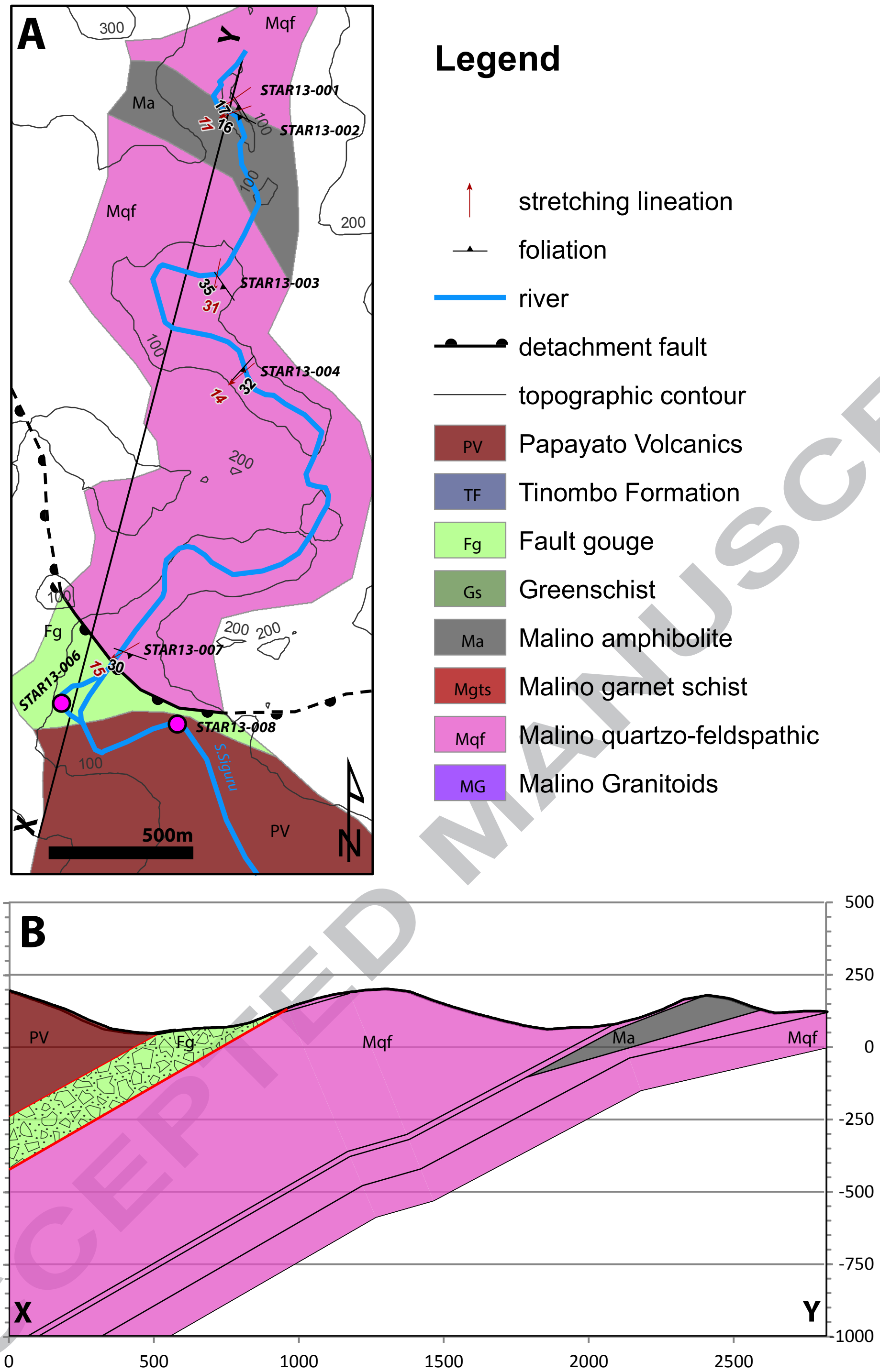

Figure 12

Figure 13

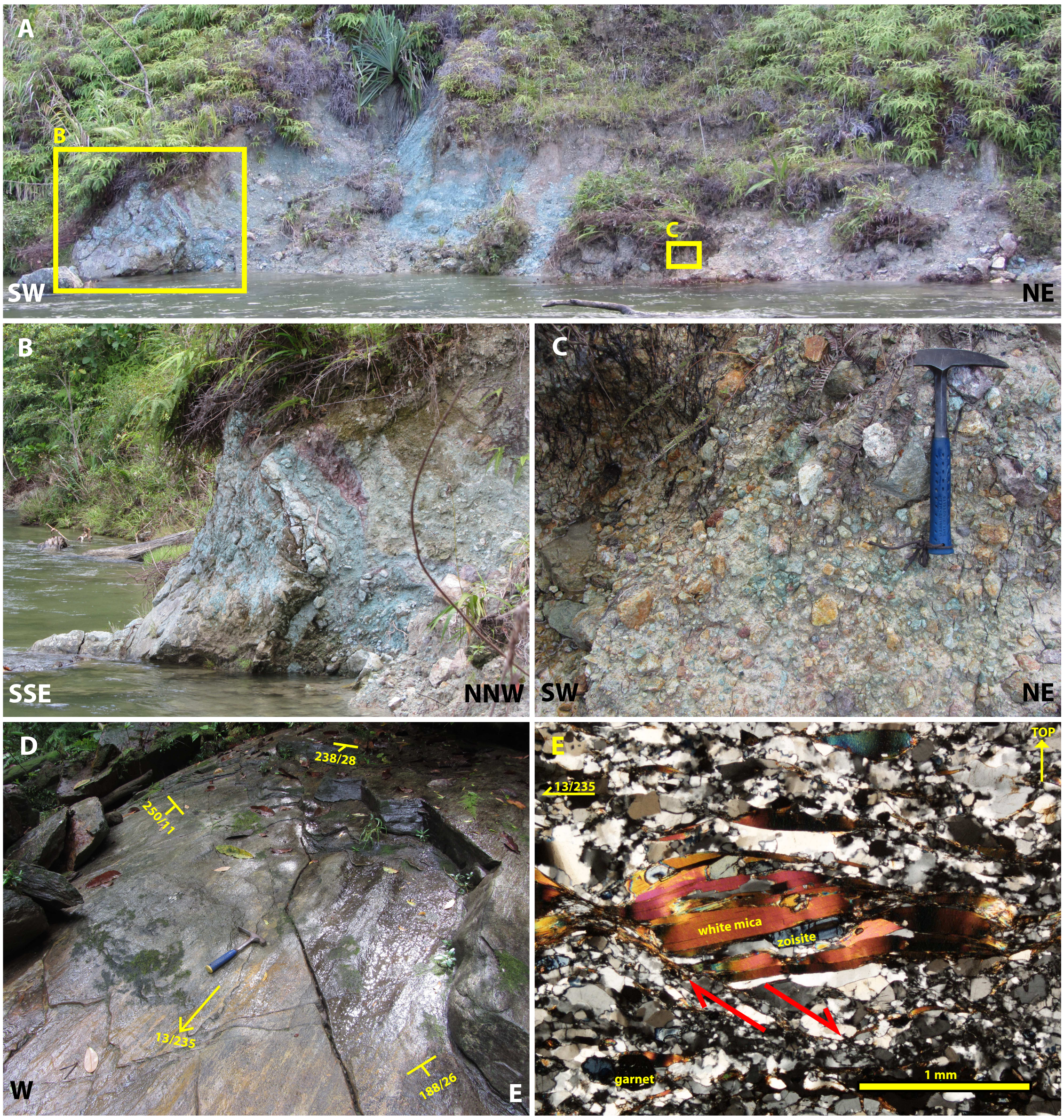

Figure 13

Figure 14

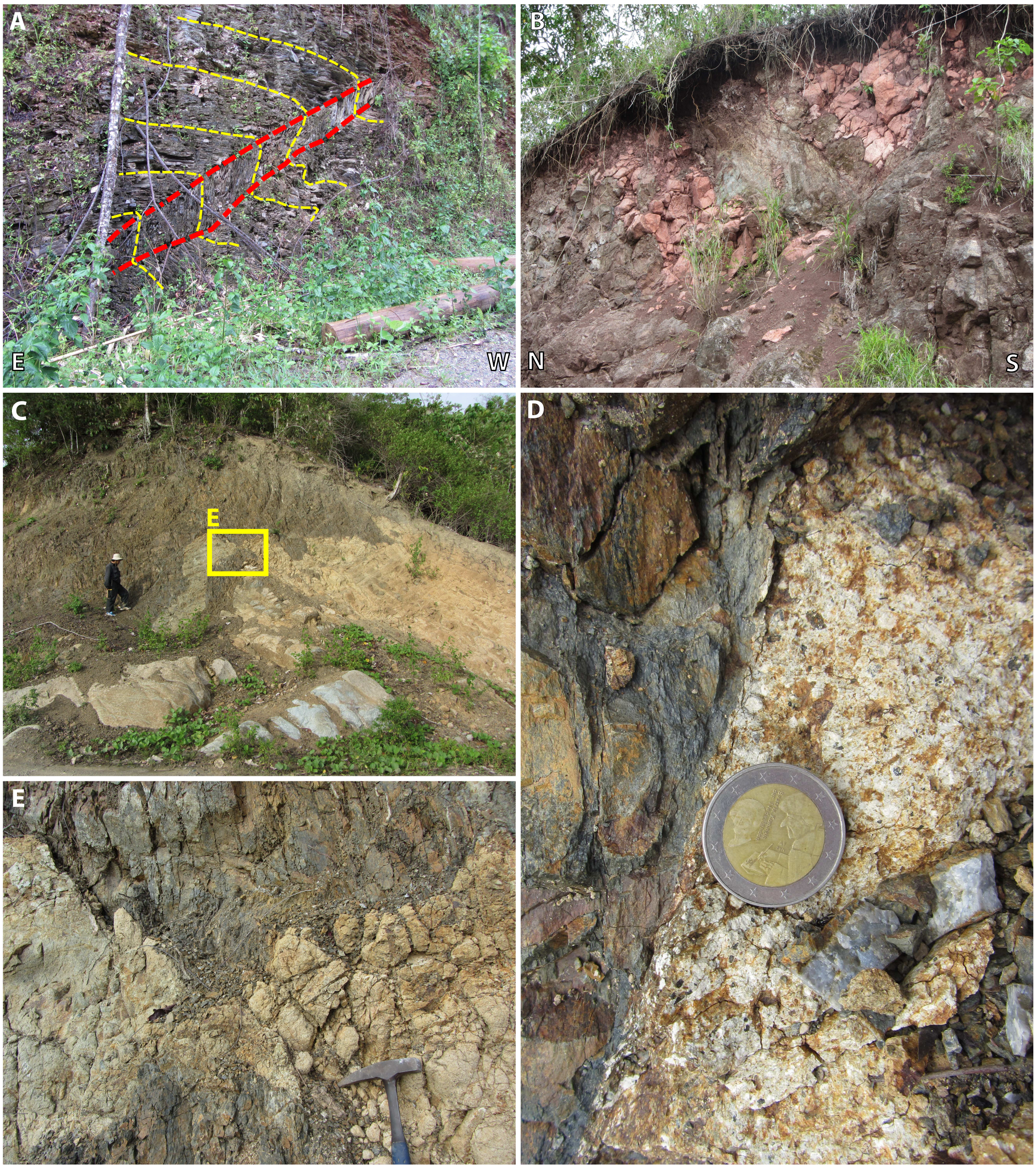

Figure 14

Figure 15

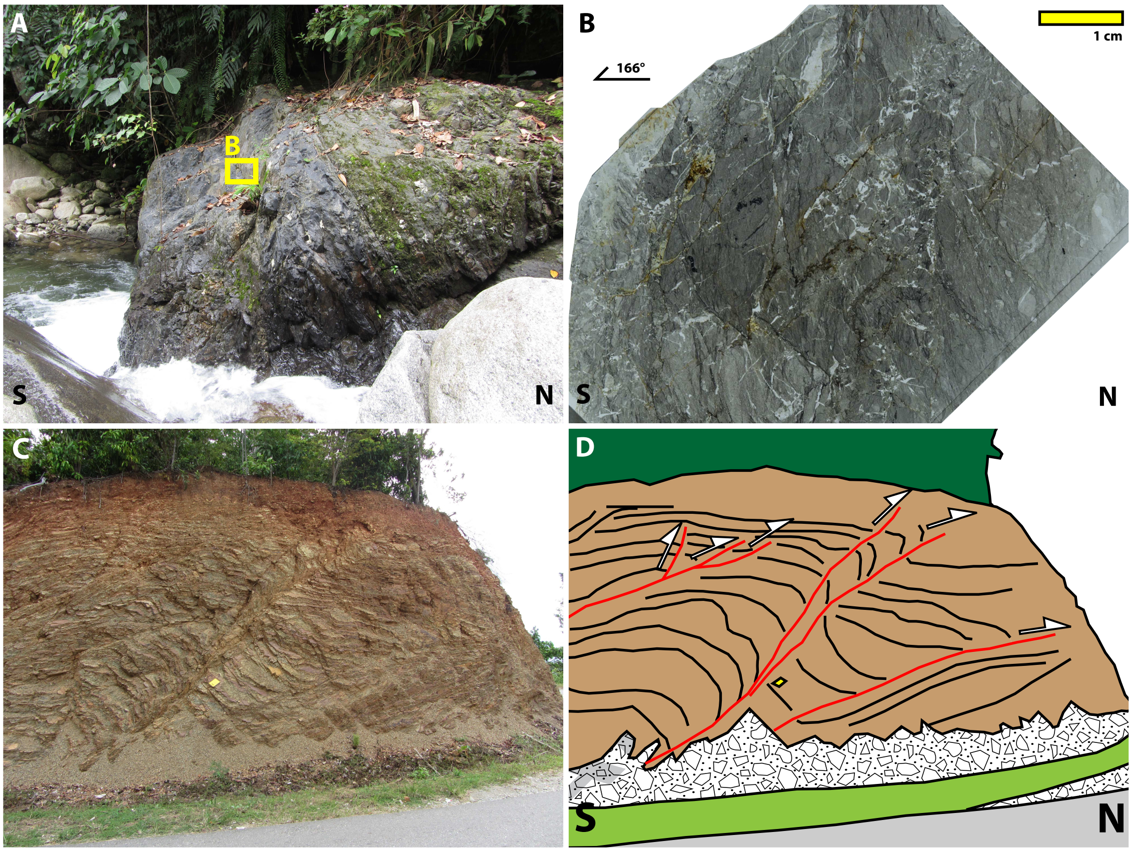

Figure 15

Figure 16

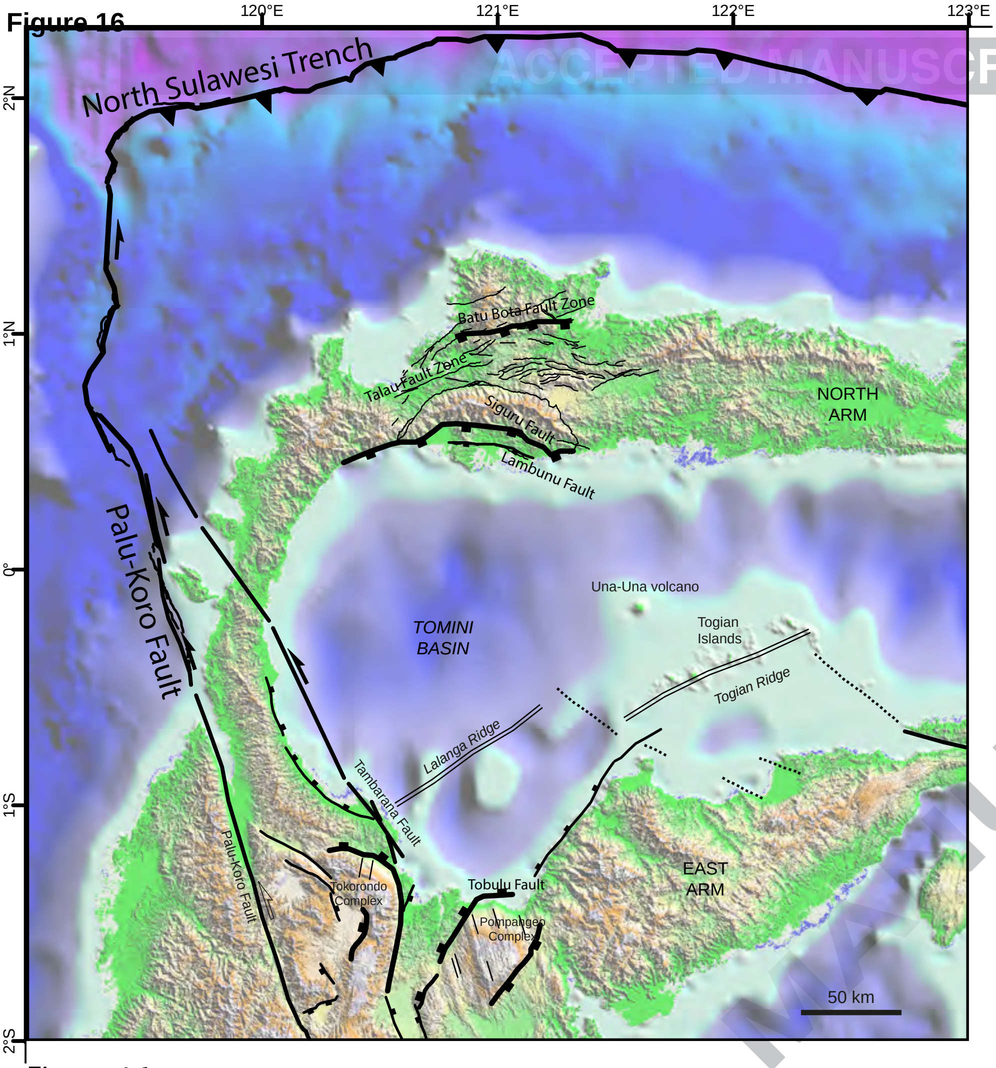

Figure 16

ACCEPTED MANUSCRIPT

Figure 17

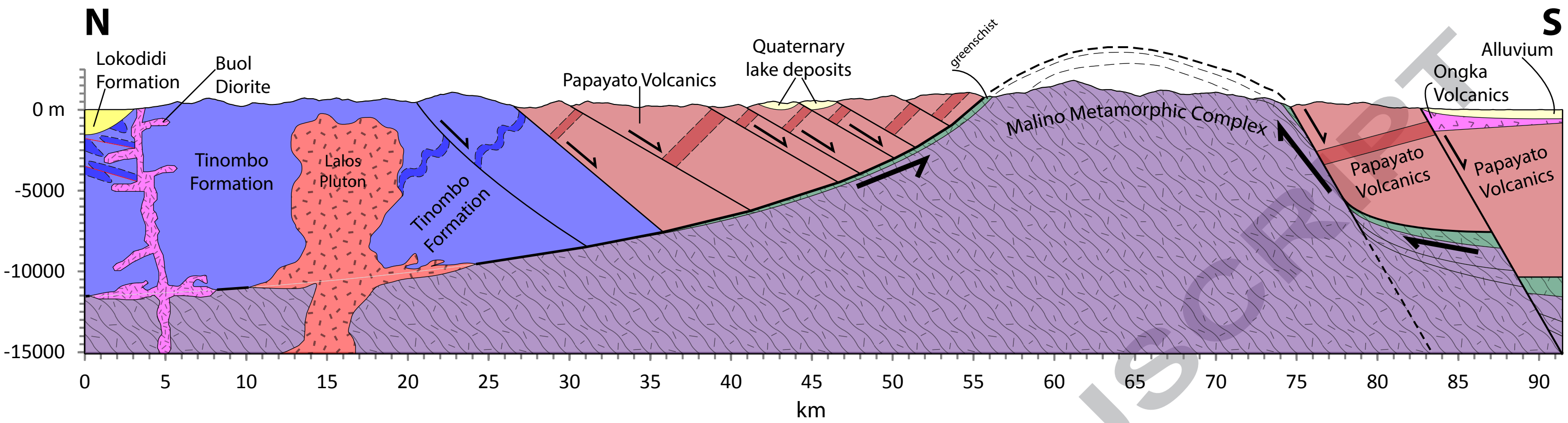

Figure 17

Table 1

Sample	Latitude	Longitude	Microfacies	components	Depositional environment	Age range	Formation
STAR12-312A	0.9118	120.8586	Micritic packstone of planktonic foraminifera	Dentoglobigerna venezuelana, Turborotalia pomeroli, Globoquadrina spp., Dentoglobigerina tripartitaDentoglobigerina pseudovenezuelana, Globigerina spp., Dentoglobigerina spp.	Inner neritic	Late Middle Eocene-Late Eocene, P14-P17.	Papayato Volcanics
STAR12-355	0.9983	121.2132	Wackestone of benthic foraminifera with reworked micritic patches	Cycloclypeus sp., Planostegina sp., Hetersotegina (Vlerkina), Lepidocyclina stratifera, Gypsina, Miogypsina tani, Victoriella sp, Elphidium sp., small miliolid, fragments of Eulepidina sp., Dentoglobigerina venezuelana, Globoquadrina altispira, Lepidocyclina (Nephrolepidina) sumatrensis, Miogypsinoides dehaarti, Echinoid spp., Rodophyte spp..	Forereef environment	Late Aquitanian-Burdigalian, N5-N6, 21.0-17.2Ma	Tinombo Formation
STAR12-302	0.9037	120.8007	Grainstone with rare benthic foraminifera	Miolepidocyclina sp., fragments of Rodophytes spp.	Reefal environment	Burdigalian, N6-N8a, 21.0-15.9	Tinombo Formation
STAR12-349B	0.9818	121.3384	Wackestone of planktonic	Globigerina sp., Globigerinoides trilobus,	Inner neritic	Late Pliocene - Early	Buol Beds

			foraminifera	Globigerinoides quadrilobatus, Truncorotalodes tosaensis, Amphistegina sp.,		Pleistocene (N21-N22)	
STAR12-328A	1.2323	121.2772	Packstone of planktonic foraminifera	Globoquadrina altispira, Globigerinoides sacculifer, Globorotalia lenguaensis, Planorbulinella larvata, Globoquadrina sp., Globigerinoides spp., Bolivina sp., Globorotalia menardii, Orbulina suturalis, Gypsina sp., Cycloclypeus sp., Amphistegina sp., Elphidium sp., Sphaeroidinella subdehiscens, Globigerinoides trilobus, Gypsina spp., Rodophyte spp.	Forereef environment	Tortonian (N14-N16)	Lokodidi Formation
STAR12-328B	1.2323	121.2772	Packstone of planktonic foraminifera	Goborotalia scitula, Globoquadrina dehiscens, Quasirotalia sp., Globorotalia margaritae, Sphaeroidinella dehiscens, Orbulina suturalis, Globorotalia menardii, Globorotalia tumida, Globorotalia inflata, Globigerinoides	Forereef environment	Early Pliocene (N19)	Lokodidi Formation

				quadrilobatus, Globigerinoides spp., Globigerinoides trilobus, Planorbulinella larvata, Amphistegina spp., Gypsina spp., Rodophyte spp.			
STAR12-335	1.199	121.4151	Packstone of planktonic foraminifera	Globorotalia margaritae, Sphaeroidinella dehiscens, Globigerinoides trilobus, Globigerinoides quadrilobatus, Globorotalia spp., Paraglobolrotalia sp., Gypsina sp., Marginopora vertebralis, Rodophyte spp., Barnacles spp., Orbulina suturalis, Amphistegina spp., Gypsina spp.	Forereef environment	Early Pliocene (N19)	Coral Limestone
STAR12-322	1.286	121.0868	Packstone of algae and benthic foraminifera	Archaias sp., miliolid sp., Planorbulinella larvata, Echinoid spp., Textularia sp., , miliolid spp. Rotalia sp., Gypsina spp., Coral spp., Rodophyte spp., Gastropod spp.	Reefal environment	Miocene to holocene	Coral Limestone
STAR12-251	0.4999	121.402	Wackestone of very rare benthic foraminifera	Migogypsina globulina (just 2 specimens), 2 fragments of recrystallised corals	Reefal environment	Early Miocene (Burdigalian)	Reefal limestone

Graphical abstract

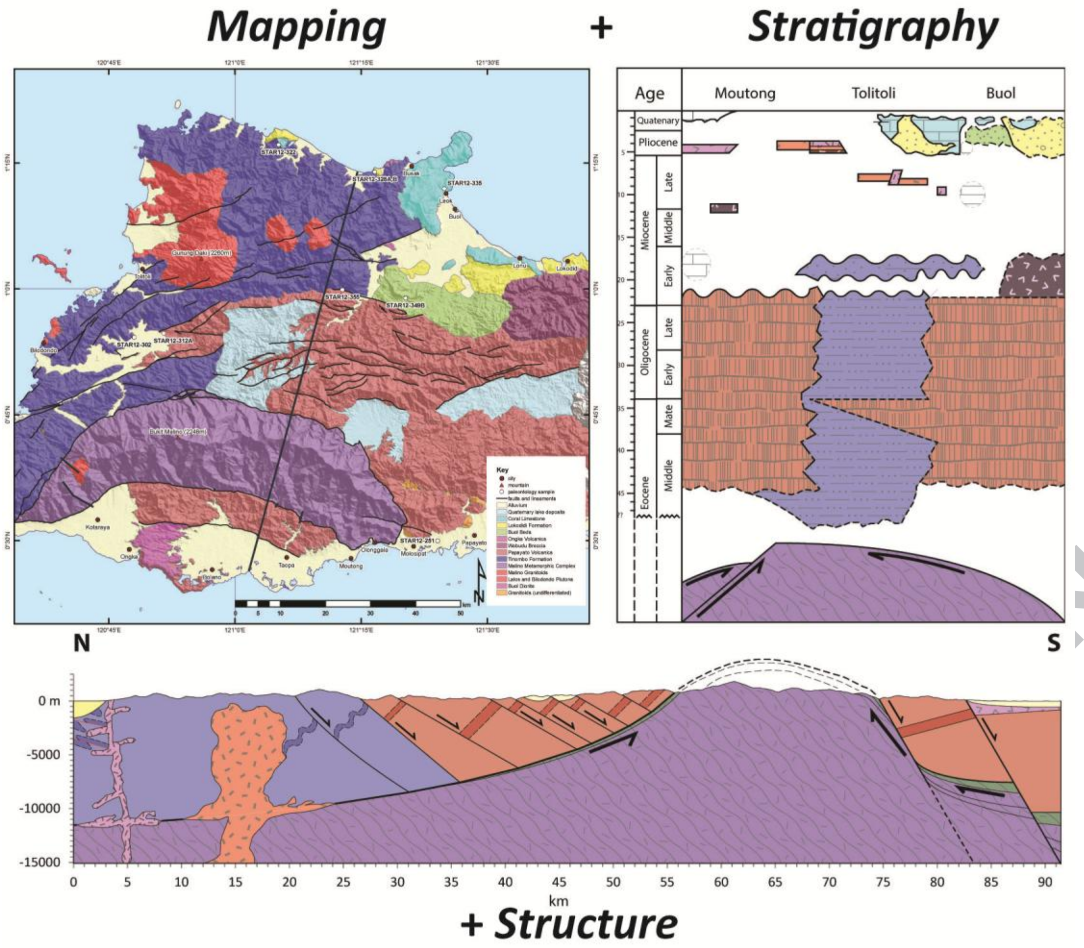

Highlights:

- New field observations, microstructural analyses and a revised stratigraphy of NW Sulawesi are presented.
- The Malino Metamorphic Complex (MMC) is metamorphic core complex. It is suggested that lithospheric extension occurred during the Early–Middle Miocene.
- The MMC was exhumed by a second phase of extensional uplift during the Late Miocene–Pliocene to present-day
- This extension is widespread and is linked to subduction rollback of the Celebes Sea